Hyperfine Structure of Many Atomic Levels of Tb^{159} and the Tb^{159} Nuclear Electric-Quadrupole Moment*

W. J. Childs

Argonne National Laboratory, Argonne, Illinois 60439
(Received 5 March 1970)

The hyperfine structure and g_J values of the 17 lowest-lying atomic levels of Tb^{159} have been measured by the atomic-beam magnetic-resonance technique. Two of the three levels studied in the $4f^9 6s^2$ configuration had not been seen before, and the present work in $4f^8 5d 6s^2$ provides the first hyperfine-structure information obtained for 11 of the 14 levels studied. The results are analyzed in detail by use of the best eigenvectors available and the effective-operator formalism. After making suitable corrections for hfs and Zeeman interactions with neighboring atomic states, values for a number of radial integrals are deduced by treating them as adjustable parameters. The value obtained for the electric-quadrupole moment of the Tb^{159} nuclear ground state is $Q(\text{Tb}^{159}) = +1.34 \pm 0.11$ b, in good agreement with earlier results. This value of Q has been corrected for Sternheimer shielding effects in both the $4f$ and $5d$ electron shells; it results from least-squares fits to the quadrupole hfs measurements in all 17 atomic states studied in both configurations.

I. INTRODUCTION

The atomic structure of Tb I has been of interest to many people in recent years. Both even-parity ($4f^8 5d 6s^2$ and $4f^8 5d^2 6s$) and odd-parity ($4f^9 6s^2$) electron configurations are known to lie low, and the atomic ground state is not yet known with certainty. A great deal of information concerning states of $4f^8 5d 6s^2$ has been obtained optically by Meinders and Klinkenberg,[1] and values of the electron g factor g_J were determined by Bender, Penselin, and Schlupmann[2] in early atomic-beam experiments for some of the lower levels. Arnoult and Gerstenkorn[3] have recently calculated eigenvectors for these levels. Much less is known experimentally about the odd-parity configuration $4f^9 6s^2$, however, although some theoretical work has been done.[4,5]

The hyperfine structure of the $4f^8 5d 6s^2$ $^8 G_{15/2, 13/2, 11/2}$ states was examined optically by Arnoult and Gerstenkorn,[3] and with the atomic-beam magnetic-resonance technique by Chan and Unsworth[6]; these results led to a determination of the magnetic-dipole and electric-quadrupole moments of the Tb^{159} nuclear ground state. The value of the dipole moment has been measured with high precision by Baker *et al.*[7] References to various determinations of these moments are given by Fuller and Cohen.[8]

The present research was undertaken because it appeared that the hyperfine interactions could well be used for a sensitive study of the properties of a large number of levels known to lie low enough in Tb to be populated thermally in an atomic beam. The atomic-beam magnetic-resonance technique was used, and the hyperfine and

Zeeman properties of 17 low-lying states (three in the $4f^9 6s^2$ configuration and 14 in $4f^8 5d 6s^2$) were observed. The results are analyzed in detail.

After correction for Sternheimer[9] shielding, a value of $Q(\text{Tb}^{159})$ is extracted from fits to the quadrupole hfs measurements in all 17 of the atomic states studied. Preliminary reports on portions of the present work have been published.[10]

II. GENERAL PRINCIPLES

The apparatus used for the present experiment was a conventional "flop-in" atomic-beam magnetic-resonance machine[11] equipped with an electron-bombardment mass-spectrometric detector. The general principles of the technique have been described many times[12] and will not be repeated here. The particular apparatus used has also been described in detail previously.[12]

In a magnetic field H, the atomic levels between which transitions are observed are eigenvalues of the Hamiltonian

$$\mathcal{H} = \mathcal{H}_{\text{hfs}} + \mathcal{H}_Z \ , \tag{1}$$

where the hyperfine and Zeeman operators are written separately. If we admit the presence of even a high degree of configuration interaction and spin-orbit mixing, but assume that hyperfine and Zeeman interactions between atomic states (with different total electronic angular momentum J) are negligibly small, then J remains a good quantum number; and for a particular state we may write[13]

$$\mathcal{H}_{\text{hfs}} = hA\vec{I} \cdot \vec{J} + hB\left(\frac{\frac{3}{2}\vec{I} \cdot \vec{J}(2\vec{I} \cdot \vec{J} + 1) - I(I+1)J(J+1)}{2I(2I-1)J(2J-1)} \right)$$

$$+\frac{hC}{I(I-1)(2I-1)J(J-1)(2J-1)}\ \tfrac{5}{4}\{8(\vec{\mathrm{I}}\cdot\vec{\mathrm{J}})^3$$

$$+16(\vec{\mathrm{I}}\cdot\vec{\mathrm{J}})^2+\tfrac{8}{5}(\vec{\mathrm{I}}\cdot\vec{\mathrm{J}})[-3I(I+1)J(J+1)+I(I+1)$$

$$+J(J+1)+3]-4I(I+1)J(J+1)\}\ ,\qquad(2)$$

$$\mathcal{K}_Z=\mu_B H(g_J J_z+g_I I_z)\ ,\qquad(3)$$

where h and μ_B are Planck's constant and the
Bohr magneton; $\vec{\mathrm{I}}$ and $\vec{\mathrm{J}}$ are the nuclear and elec-
tronic angular momentum operators; $A, B,$ and
C are the magnetic-dipole, electric-quadrupole,
and magnetic-octupole hyperfine-interaction con-
stants; and g_J and g_I are the electron and nuclear
g factors. Hyperfine-interaction terms of higher
order than magnetic octupole have been dropped
from Eq. (2) as being smaller than the present
experimental uncertainties.

The resonance frequency ν observed for a tran-
sition at field H should be derivable from Eqs.
(1)-(3) to a very high accuracy, even for an atom
as far removed from the LS limit as Tb. The
principal source of error in Eqs. (2) and (3) is the
failure to take account of the fact that hyperfine
and Zeeman interactions can mix states of differ-
ent J. These effects, are treated in detail in
Sec. IV F.

Another limitation of Eqs. (2) and (3) is the fact
that although they apply to any atomic state and
therefore make possible extraction of values of
$A, B, C,$ and g_J for that state, they give no infor-
mation concerning the way in which these quanti-
ties vary from state to state. A treatment of the
two interactions more fundamental than that of
Eqs. (2) and (3) is therefore desirable, and is
given in Sec. IV D.

Two computer programs based on Eqs. (1)-(3)
were essential[14] in the data-taking stages of the
experiment. The first typically varies the quan-
tities $A, B,$ and g_J to make a least-squares fit of
the appropriate eigenvalue differences $\nu=(E_1$
$-E_2)/h$ to any set of resonance frequencies mea-
sured at known values of H. The second program,
using the values of $A, B,$ and g_J found above (or
from other considerations), calculates any desired
transition frequencies at a sequence of values of
H. These programs were used repeatedly; the
difficulties discussed above (stemming from the
breakdown of J as a good quantum number) led to
poor values of χ^2 in the fitting program only for
the states ${}^8G_{5/2,3/2}$.

III. EXPERIMENTAL CONSIDERATIONS

A. Apparatus

The atomic beam of Tb was produced by elec-
tron bombardment of a Ta oven equipped with a
sharp-lipped Ta inner crucible to limit creep.
The Tb^{159} atoms effused through a 0.010×0.250-
in. slit at a temperature of about 1600°C to form
the beam. It was possible to remove the oven lid
repeatedly in order to refill the oven; and a dif-
ferentially pumped, pneumatically driven oven-
loading system made it possible to reload without
breaking the vacuum.

The homogeneous C field, in which the rf tran-
sitions took place, was set to the desired intensity
by observing transitions in a beam of K^{39} from an
auxiliary oven system. In searching for Tb res-
onances at a known value of H, the rf applied was
swept repeatedly, usually in 10-kHz steps, through
the frequency range of interest.[15] The electron-
multiplier pulses due to detected atoms were am-
plified, scaled down a factor of 10 by a 100-MHz
scaler, and then fed into a multichannel scaler
whose address was advanced in synchronism with
the rf sweep. While collecting data, the improve-
ment in the signal-to-noise ratio for a resonance
could be observed on an oscilloscope screen, and
the accumulation of data stopped when the pattern
appeared satisfactory. Because thermal excitation
was the only source of population of the metastable
states observed, the intensity of the transitions in
excited states fell off rapidly with excitation. For
transitions which are only a few percent as in-
tense as those in the ground state, the occurrence
of a nonrandom change in counting rate while the
scanning system is sweeping across only a few
channels can destroy data which has been collect-
ing over a long period of time. A digital filter[16]
was employed to eliminate or greatly reduce such
nonrandom noise. In effect, if the number of pul-
ses arriving at a given channel in the course of a
sweep differs from the average of the counts added
to each channel on the previous sweep by a set
amount (such as 3 standard deviations, for exam-
ple), then the old average is added to the channel
contents instead of the new number. The filter,
which must be shut off while scanning rf regions
containing strong signals, was essential for work
on the weaker states.

The swept rf was produced by mixing a swept
30-MHz signal and a second crystal-controlled
fixed frequency. The first signal could be swept,
in steps of 1, 2, 5, or 10 kHz, from 30 MHz to any
frequency up to 31 MHz, and was produced by a
Hewlett-Packard synthesizer. The fixed-frequen-
cy source for the 0–1000-MHz range was a Solar-
tron precision signal generator with the appropri-
ate frequency multipliers and amplifiers; and for
1–8-GHz, magnetrons and a backward-wave os-
cillator were phase locked to the Solartron. Fre-
quencies from 0 to 4 GHz were measured with an
Eldorado counter, and those from 4 to 8 GHz were

TABLE I. The low-lying atomic levels of Tb I. The relative excitation energies of the $4f^9 6s^2$ levels are from calculations of Ref. 4; it is not known where they lie relative to those of $4f^8 5d 6s^2$. The labeling of the states of $4f^8 5d 6s^2$ follows Ref. 1; because of the strong departure of many of the $4f^8 5d 6s^2$ states from the LS limit, the L (and to a lesser extent the S) value assigned, though useful, is physically meaningless. The Boltzmann factors are calculated for $T \approx 1600\,°C$, for which the Tb vapor pressure is 0.1 Torr.

Relative excitation energy (cm⁻¹)	Electron configuration	Designation of state	Relative Boltzmann factor
0	$4f^9 6s^2$	$^6H_{15/2}$	1.000
(2810)	$4f^9 6s^2$	$^6H_{13/2}$	0.118
(4792)	$4f^9 6s^2$	$^6H_{11/2}$	0.026
0	$4f^8 5d 6s^2$	$^8G_{13/2}$	1.000
177	$4f^8 5d 6s^2$	$^8G_{15/2}$	0.874
224	$4f^8 5d 6s^2$	$^8G_{11/2}$	0.843
1086	$4f^8 5d 6s^2$	$^8G_{9/2}$	0.437
2025	$4f^8 5d 6s^2$	$^8D_{11/2}$	0.214
2134	$4f^8 5d 6s^2$	$^8G_{7/2}$	0.197
2555	$4f^8 5d 6s^2$	$^8D_{9/2}$	0.143
2889	$4f^8 5d 6s^2$	$^8G_{5/2}$	0.111
3420	$4f^8 5d 6s^2$	$^8G_{3/2}$	0.074
3434	$4f^8 5d 6s^2$	$^8F_{13/2}$	0.073
3534	$4f^8 5d 6s^2$	$^8D_{7/2}$	0.068
3733	$4f^8 5d 6s^2$	$^8G_{1/2}$	0.058
4361	$4f^8 5d 6s^2$	$^8H_{17/2}$	0.036
4410	$4f^8 5d 6s^2$	$^8D_{5/2}$	0.035
5068	$4f^8 5d 6s^2$	$^8F_{11/2}$	0.021
5139	$4f^8 5d 6s^2$	$^8H_{15/2}$	0.020

scaled down by a factor of 1000 by a Hewlett-Packard frequency divider before measurement.

B. Experimental Procedure

Table I lists the known and projected levels of Tb I which lie below about 5000 cm⁻¹. The relative energies and designations of the levels of the $4f^8 5d 6s^2$ configuration are from Meinders and Klinkenberg, [1] and the relative energies for the $4f^9 6s^2$ states are from calculations of Conway and Wybourne. [4] It is not yet known with certainty whether the atomic ground state is $4f^8 5d 6s^2\, ^8G_{13/2}$ or $4f^9 6s^2\, ^6H_{15/2}$, or what the relative spacing is. The identity of the ground state, and the properties of the states in general, will be discussed in Sec. IV A. Boltzmann factors, calculated for the oven temperature of 1600°C, are included to indicate approximately the expected relative intensities of the transitions (between individual magnetic substates) which are observed in the experiment. The J values range from $\frac{1}{2}$ to $\frac{17}{2}$; and for $I(\mathrm{Tb}^{159})$ $= \frac{3}{2}$, [8] there are four $\Delta F = 0$, $\Delta M_F = \pm 1$ transitions which can be refocused for each state with $J > \frac{5}{2}$. In addition, the application of too much rf power

may induce a number of multiple-quantum transitions ($|\Delta M_F| \geq 2$) with intensities comparable to those for single-quantum transitions, and the intensities of these transitions may be enhanced by slight misalignment of the atomic beam. Even at low rf power, such multiple-quantum transitions in strong states may be comparable in intensity to the normal single-quantum transitions in less populated states.

It is clear that at small values of H, the number of transitions expected within a given frequency range will be very large. Bender, Penselin, and Schlupmann[2] found a continuous string of unresolved resonances from 10 to 20 MHz in Tb^{159} at $H = 7$ G. Figure 1 shows a typical 1-MHz sweep at 20 G. Even at this field, although half the scan reveals no resonance, five transitions are unresolved in the other half. In the identification scheme used for the single-quantum $\Delta F = 0$, $\Delta M_F = \pm 1$ transitions, α denotes $F = I + J$, β denotes $F = I + J - 1$, etc., where $\vec{F} = \vec{I} + \vec{J}$ is the total angular momentum of the atom. Figures 2 and 3 show that even at $H = 50$ G, rf sweeps of $\frac{1}{2}$ MHz are likely to reveal more than one transition. The failure of the relative intensities of the transitions shown in Figs. 1–3 to correspond exactly to the relative Boltzmann factors of Table I is due to the dependence of the transition probability on other quantities such as rf power level, g_J, and angular momentum considerations.
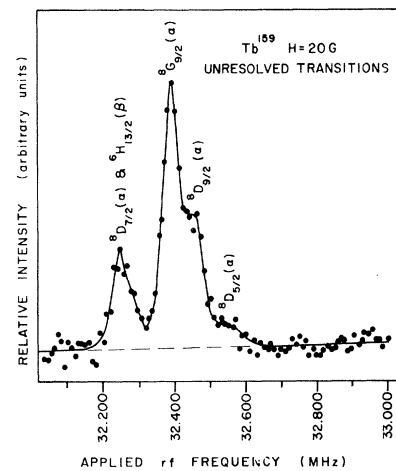
FIG. 1. Typical rf spectrum resulting from a 1-MHz sweep at $H = 20$ G. As seen from the smooth curve drawn through the experimental points, the spectrum appears to consist of two resonances, possibly distorted by excessive rf power. It is known, however, that resonances occur in the swept region in five low-lying atomic states as indicated. The identification of resonances and measurement of transition frequencies at such low fields is difficult in an atom as complex as Tb^{159}.
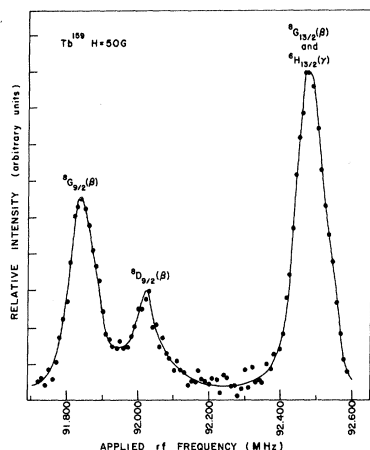
FIG. 2. Resolution of transitions with identical F, M, F', M' values in the $^8G_{9/2}$ and $^8D_{9/2}$ states at 50 G. The value of g_J differs by less than 0.2% between the two states. The two transitions that form the single peak at the right are resolved only for $H \geq 125$ G.

It is clear that in measuring the hfs of the various low-lying states, the well-populated lower levels should be studied first. Bender, Penselin, and Schlupmann[2] were able to make preliminary measurements of the g_J values of five levels, and Unsworth and Chan[6] made detailed measurements of the hfs and g values of the $4f^9 6s^2$ $^6H_{15/2}$ and the $4f^8 5d 6s^2$ $^8G_{15/2, \, 13/2, \, 11/2}$ states. The very valuable
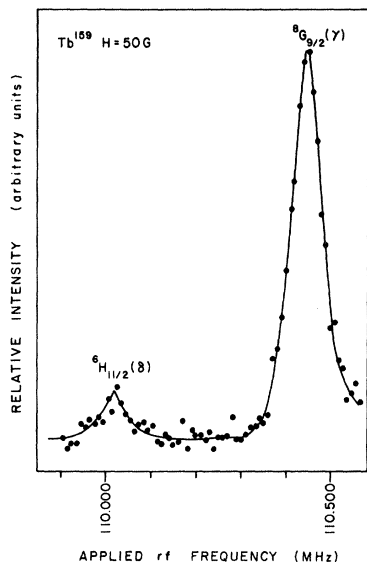
FIG. 3. Appearance of a $\Delta F = 0$ transition in the $4f^9 6s^2$ $^6H_{11/2}$ state at 50 G. Although the excitation energy of this state is not known, it was among the least populated of those studied. With longer counting times, the signal-to-noise ratio could be increased a little over that shown, but it would be difficult to study states lying appreciably higher without modification of the apparatus.
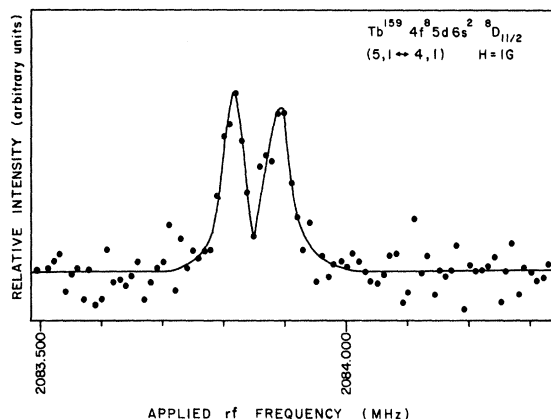
FIG. 4. Appearance of a $\Delta F = \pm 1$ transition in the $^8D_{11/2}$ state at 1 G. The origin of the line shape is discussed in the text. The signal-to-noise ratio can be improved by longer counting times.

work of Meinders and Klinkenberg[1] and of Arnoult and Gerstenkorn[3] will be described in Sec. IV.

The procedure followed in the present experiment was to calculate the $\Delta F = 0$ transition frequencies for the state in question at a number of values of H, using Klinkenberg's optical g_J value[1] and the best estimate of the hyperfine-interaction constants A and B which could be made from the eigenvectors of Arnoult and Gerstenkorn.[3] If any one of these calculated resonance frequencies was sufficiently isolated from other resonances, both known and projected, at any field $H \leq 20$ G, it was searched for. If found, a more precise value of g_J could be deduced and used to predict the frequencies at higher fields.

For some states, the calculated resonance frequencies all lay so near those of stronger transitions for $H \leq 20$ G that this procedure could not be followed. Searching for a transition in a previously unobserved state at fields much above 20 G was tedious and sometimes unrewarding because of the very large uncertainty in the predicted frequency. The two states $4f^8 5d 6s^{28} G_{9/2}$ and $^8D_{9/2}$ were particularly troublesome in that all quantum numbers determining transition frequency are identical for the two states, and in addition, the g_J values happen to differ by less than 0.2%. Figure 2 shows the resolution of the β transition in the two levels at 50 G. Figure 1 shows the situation for the α transition at 20 G; the curve through the points could be redrawn so as to give only a hint of the $^8D_{9/2}$ transition.

As transitions were observed at higher and higher fields, better and better estimates could be made of g_J and of the values of the hyperfine-interaction constants A and B, or equivalently, of the zero-field hyperfine intervals. When these

intervals could be predicted well enough (say to within ±2 MHz), the $\Delta F = \pm 1$ transitions were searched for directly, usually at 1 G. Figure 4 shows such a transition in the $4f^85d6s^2$ $^8D_{11/2}$ state as observed at 1 G. The dip in the center of the line is due to the presence of two nearby regions of rf field, 180° out of phase. The experimental and theoretical considerations relevant to such line shapes have been discussed before.[17] Certain $\Delta F = \pm 1$ transition frequencies were also measured at values of H (typically above 100 G) for which $\partial \nu / \partial H = 0$.

The observed resonance frequencies are listed in Table II together with the differences between the observed and calculated frequencies. The calculated transition frequencies used in obtaining the residuals include corrections for the effects of hyperfine and Zeeman interactions with other atomic states. The procedures used in making the corrections will be discussed in Sec. IV F; the effects were most pronounced for the $^8G_{5/2,3/2,1/2}$ states.

The evaluation of the hyperfine-interaction constants is complete for 15 states in the sense that all zero-field hyperfine intervals have been measured. The single $\Delta F = \pm 1$ interval in the $^8G_{1/2}$ state was not observed; the failure to see it may be due either to inadequate rf power at $\Delta \nu \approx 5170$ MHz or to inaccuracy in this estimate of the transition frequency. None of the $\Delta F = \pm 1$ transitions were searched for in the $4f^96s^2$ $^6H_{11/2}$ state, primarily because the very low intensity for this state precluded adequately precise estimates of the zero-field intervals.

Two transitions that were repeatedly observed with low intensities are listed at the bottom of Table II. They were seen at low field while searching for the expected $F = 1 \rightarrow 2$ transitions in the $4f^85d6s^2$ $^8G_{1/2}$ state and were at first assumed to be these transitions. Several such resonances should have appeared close together at such small values of H, however, and the observed transition appeared to have no near neighbors. Furthermore, if the resonances observed at 1 and 2 G are of the same transition, as appears most likely, its observed field dependence

$$\frac{\partial \nu}{\partial H} = +0.153(15)\,\text{MHz/G}$$

is considerably less than the expected $\partial \nu / \partial H$ for any of the $F = 1 \rightarrow 2$ transitions in $^8G_{1/2}$, except for $(2, 0 \rightarrow 1, 0)$ for which $\partial \nu / \partial H$ should be zero. The observed resonances are consistent in both transition frequency ν and $\partial \nu / \partial H$ with predictions for the $(9 - 1 \rightarrow 8, -1)$ transition in the state $4f^85d6s^2$ $^8H_{15/2}$ (5139 cm^{-1}) on the basis of the Arnoult-Gerstenkorn[3] eigenvectors and the optically ob-

TABLE II. Resonance frequencies measured for transitions in Tb[159]. The theoretical resonance frequency used in evaluating the residuals in the right-hand column includes corrections for hyperfine and Zeeman interactions with other atomic states. The values of A, B, C, g_J, and χ^2 corresponding to these residuals are given in the two right-hand columns of Table III. The identification of the final two observations in Table II is tentative, and is discussed in the text.

Configuration and state designation	H (G)	Transition $(F, M \rightarrow F', M')$	Observed resonance frequency (MHz)	$\nu^{obs} - \nu^{calc}$ (kHz)
$4f^96s^2\,^6H_{15/2}$	100	$(9, -1 \rightarrow 9, -2)$	154.660(15)	-15
	100	$(8, \ 0 \rightarrow 8, -1)$	170.069(15)	-23
	100	$(7, \ 1 \rightarrow 7, \ 0)$	192.086(13)	-2
	100	$(6, \ 2 \rightarrow 6, \ 1)$	225.634(13)	-15
	400	$(9, -1 \rightarrow 9, -2)$	620.543(17)	-8
	400	$(8, \ 0 \rightarrow 8, -1)$	682.257(15)	11
	400	$(7, \ 1 \rightarrow 7, \ 0)$	769.937(20)	10
	400	$(6, \ 2 \rightarrow 6, \ 1)$	904.373(20)	19
	400	$(9, -1 \rightarrow 9, -2)$	620.553(15)	2
	400	$(8, \ 0 \rightarrow 8, -1)$	682.229(15)	-17
	400	$(7, \ 1 \rightarrow 7, \ 0)$	769.923(15)	-4
	400	$(6, \ 2 \rightarrow 6, \ 1)$	904.362(17)	8
	1	$(9, -1 \rightarrow 8, -1)$	6933.622(12)	0
	1	$(8, \ 0 \rightarrow 7, \ 0)$	5224.374(12)	-9
	2	$(8, \ 0 \rightarrow 7, \ 0)$	5224.385(4)	1
	1	$(7, \ 1 \rightarrow 6, \ 1)$	3846.291(12)	-3
	190	$(7, \ 1 \rightarrow 6, \ 1)$	3814.870(12)	3
$^6H_{13/2}$	10	$(7, \ 0 \rightarrow 7, -1)$	16.108(10)	-1
	10	$(5, \ 2 \rightarrow 5, \ 1)$	22.338(15)	0
	20	$(8, -1 \rightarrow 8, -2)$	29.043(11)	12
	50	$(8, -1 \rightarrow 8, -2)$	72.611(10)	10
	50	$(8, -1 \rightarrow 8, -2)$	72.582(13)	-19
	50	$(7, \ 0 \rightarrow 7, -1)$	80.533(20)	-31
	100	$(8, -1 \rightarrow 8, -2)$	145.283(25)	-3
	100	$(8, -1 \rightarrow 8, -2)$	145.284(25)	-2
	100	$(7, \ 0 \rightarrow 7, -1)$	161.197(12)	6
	100	$(7, \ 0 \rightarrow 7, -1)$	161.193(16)	2
	100	$(7, \ 0 \rightarrow 7, -1)$	161.224(20)	33
	100	$(5, \ 2 \rightarrow 5, \ 1)$	223.926(12)	6
	100	$(5, \ 2 \rightarrow 5, \ 1)$	223.938(20)	18
	200	$(8, -1 \rightarrow 8, -2)$	290.933(20)	2
	200	$(7, \ 0 \rightarrow 7, -1)$	322.696(13)	-12
	200	$(5, \ 2 \rightarrow 5, \ 1)$	448.686(11)	-13
	400	$(8, -1 \rightarrow 8, -2)$	583.489(15)	10
	400	$(7, \ 0 \rightarrow 7, -1)$	647.269(17)	-14
	400	$(6, \ 1 \rightarrow 6, \ 0)$	742.227(20)	2
	400	$(5, \ 2 \rightarrow 5, \ 1)$	898.497(18)	-8
	1000	$(8, -1 \rightarrow 8, -2)$	1474.008(40)	21
	1000	$(7, \ 0 \rightarrow 7, -1)$	1641.098(40)	-14
	1000	$(6, \ 1 \rightarrow 6, \ 0)$	1882.479(40)	5
	1000	$(5, \ 2 \rightarrow 5, \ 1)$	2213.270(50)	67
	1	$(8, -1 \rightarrow 7, -1)$	6182.130(20)	0
	1	$(7, \ 0 \rightarrow 6, \ 0)$	4623.245(15)	-2
	2	$(7, \ 0 \rightarrow 6, \ 0)$	4623.250(16)	2
	1	$(6, \ 1 \rightarrow 5, \ 1)$	3378.552(15)	-15
	200	$(6, \ 1 \rightarrow 5, \ 1)$	3340.253(20)	27
$^6H_{11/2}$	10	$(7, -1 \rightarrow 7, -2)$	13.297(17)	33
	50	$(7, -1 \rightarrow 7, -2)$	66.390(20)	31
	100	$(7, -1 \rightarrow 7, -2)$	132.845(13)	26
	200	$(7, -1 \rightarrow 7, -2)$	266.065(14)	-3

TABLE II. *(continued)*

Configuration and state designation	H (G)	Transition $(F, M \leftrightarrow F', M')$	Observed resonance frequency (MHz)	$\nu^{obs} - \nu^{calc}$ (kHz)
	400	(7, −1 ↔ 7, −2)	534.030(20)	− 5
	800	(7, −1 ↔ 7, −2)	1076.960(50)	13
	10	(6, 0 ↔ 6, −1)	14.895(20)	23
	50	(6, 0 ↔ 6, −1)	74.393(15)	6
	200	(6, 0 ↔ 6, −1)	298.150(15)	20
	400	(6, 0 ↔ 6, −1)	598.575(28)	− 24
	800	(6, 0 ↔ 6, −1)	1211.005(60)	− 32
	50	(5, 1 ↔ 5, 0)	87.230(18)	35
	200	(5, 1 ↔ 5, 0)	348.955(20)	− 2
	400	(5, 1 ↔ 5, 0)	700.583(30)	− 26
	50	(4, 2 ↔ 4, 1)	110.017(15)	33
	100	(4, 2 ↔ 4, 1)	220.400(25)	3
	400	(4, 2 ↔ 4, 1)	886.657(25)	− 14
	800	(4, 2 ↔ 4, 1)	1757.520(50)	− 25
$4f^8 5d 6s^2$ $^8G_{13/2}$	100	(8, −1 ↔ 8, −2)	166.803(13)	− 9
	100	(5, 2 ↔ 5, 1)	257.193(15)	− 12
	400	(8, −1 ↔ 8, −2)	671.517(13)	1
	400	(7, 0 ↔ 7, −1)	745.514(15)	− 6
	400	(6, 1 ↔ 6, 0)	855.260(17)	7
	400	(5, 2 ↔ 5, 1)	1028.870(20)	5
	1	(8, −1 ↔ 7, −1)	4829.526(11)	0
	1	(7, 0 ↔ 6, 0)	3600.363(10)	0
	1	(6, 1 ↔ 5, 1)	2621.140(10)	− 4
	2	(6, 1 ↔ 5, 1)	2620.705(10)	− 4
	135	(6, 1 ↔ 5, 1)	2591.625(12)	12
$^8G_{15/2}$	100	(9, −1 ↔ 9, −2)	169.994(20)	− 69
	100	(8, 0 ↔ 8, −1)	186.993(15)	− 1
	100	(6, 2 ↔ 6, 1)	248.178(14)	− 3
	200	(8, 0 ↔ 8, −1)	374.527(15)	7
	200	(6, 2 ↔ 6, 1)	496.899(15)	− 23
	400	(9, −1 ↔ 9, −2)	683.721(20)	3
	400	(8, 0 ↔ 8, −1)	752.300(15)	2
	400	(7, 1 ↔ 7, 0)	849.380(17)	17
	400	(6, 2 ↔ 6, 1)	991.443(18)	2
	1	(9, −1 ↔ 8, −1)	946.533(11)	0
	1	(8, 0 ↔ 7, 0)	3649.278(15)	0
	1	(7, 1 ↔ 6, 1)	2615.575(11)	− 2
	2	(7, 1 ↔ 6, 1)	2615.208(11)	− 10
	115	(7, 1 ↔ 6, 1)	2594.770(12)	14
$^8G_{11/2}$	100	(7, −1 ↔ 7, −2)	167.145(20)	− 12
	100	(6, 0 ↔ 6, −1)	187.320(20)	− 11
	100	(5, 1 ↔ 5, 0)	219.310(20)	− 8
	100	(4, 2 ↔ 4, 1)	277.720(20)	− 19
	200	(7, −1 ↔ 7, −2)	335.175(20)	− 21
	200	(6, 0 ↔ 6, −1)	375.710(20)	− 27
	200	(5, 1 ↔ 5, 0)	439.775(20)	− 30
	200	(4, 2 ↔ 4, 1)	557.226(20)	− 38
	400	(7, −1 ↔ 7, −2)	674.440(20)	14
	400	(6, 0 ↔ 6, −1)	757.805(20)	5
	400	(5, 1 ↔ 5, 0)	889.580(20)	19
	400	(4, 2 ↔ 4, 1)	1110.132(20)	33
	400	(7, −1 ↔ 7, −2)	674.422(17)	− 4

TABLE II. *(continued)*

Configuration and state designation	H (G)	Transition $(F, M \leftrightarrow F', M')$	Observed resonance frequency (MHz)	$\nu^{obs} - \nu^{calc}$ (kHz)
	400	(6, 0 ↔ 6, −1)	757.800(20)	0
	400	(5, 1 ↔ 5, 0)	889.560(20)	− 1
	400	(4, 2 ↔ 4, 1)	1110.102(18)	3
	1	(7, −1 ↔ 6, −1)	4672.535(10)	0
	1	(6, 0 ↔ 5, 0)	3302.833(10)	0
	1	(5, 1 ↔ 4, 1)	2256.765(8)	2
	130	(5, 1 ↔ 4, 1)	2220.445(12)	− 4
$^8G_{9/2}$	10	(6, −1 ↔ 6, −2)	16.189(12)	8
	10	(5, 0 ↔ 5, −1)	18.354(13)	16
	10	(4, 1 ↔ 4, 0)	22.118(15)	18
	10	(3, 2 ↔ 3, 1)	29.728(20)	15
	20	(5, 0 ↔ 5, −1)	36.679(13)	− 8
	20	(4, 1 ↔ 4, 0)	44.164(14)	− 22
	50	(4, 1 ↔ 4, 0)	10.430(17)	9
	50	(3, 2 ↔ 3, 1)	49.467(15)	− 21
	100	(6, −1 ↔ 6, −2)	62.315(7)	4
	100	(5, 0 ↔ 5, −1)	83.995(10)	− 2
	100	(4, 1 ↔ 4, 0)	221.116(10)	− 10
	100	(3, 2 ↔ 3, 1)	300.760(18)	− 18
	150	(4, 1 ↔ 4, 0)	332.890(25)	− 5
	150	(3, 2 ↔ 3, 1)	452.840(20)	4
	200	(6, −1 ↔ 6, −2)	325.797(20)	− 41
	200	(5, 0 ↔ 5, −1)	370.030(25)	5
	200	(4, 1 ↔ 4, 0)	446.337(18)	− 4
	200	(3, 2 ↔ 3, 1)	604.471(18)	7
	400	(6, −1 ↔ 6, −2)	657.117(15)	− 5
	400	(5, 0 ↔ 5, −1)	751.883(15)	15
	400	(4, 1 ↔ 4, 0)	920.166(20)	5
	400	(3, 2 ↔ 3, 1)	1187.830(20)	11
	1	(6, −1 ↔ 5, −1)	4458.555(11)	0
	1	(5, 0 ↔ 4, 0)	2747.086(13)	0
	1	(4, 1 ↔ 3, 1)	1563.270(10)	2
	100	(4, 1 ↔ 3, 1)	1525.690(13)	− 3
$^8D_{11/2}$	10	(7, −1 ↔ 7, −2)	16.846(17)	13
	10	(4, 2 ↔ 4, 1)	27.876(20)	7
	20	(5, 1 ↔ 5, 0)	44.264(13)	8
	100	(7, −1 ↔ 7, −2)	168.955(15)	− 13
	100	(6, 0 ↔ 6, −1)	189.112(25)	− 14
	100	(5, 1 ↔ 5, 0)	221.310(17)	− 30
	100	(7, −1 ↔ 7, −2)	168.955(15)	− 13
	100	(6, 0 ↔ 6, −1)	189.132(20)	6
	100	(5, 1 ↔ 5, 0)	221.347(20)	7
	100	(4, 2 ↔ 4, 1)	280.347(15)	− 20
	200	(7, −1 ↔ 7, −2)	339.575(17)	− 17
	200	(6, 0 ↔ 6, −1)	379.740(20)	− 10
	200	(5, 1 ↔ 5, 0)	443.836(25)	− 1
	200	(4, 2 ↔ 4, 1)	562.415(15)	7
	400	(7, −1 ↔ 7, −2)	687.039(15)	− 10
	400	(6, 0 ↔ 6, −1)	768.283(20)	39
	400	(5, 1 ↔ 5, 0)	896.620(20)	7
	400	(4, 2 ↔ 4, 1)	1117.316(25)	4
	1	(7, −1 ↔ 6, −1)	2777.218(13)	0

TABLE II. *(continued)*

Configuration and state designation	H (G)	Transition $(F, M \rightarrow F', M')$	Observed resonance frequency (MHz)	$\nu^{obs} - \nu^{calc}$ (kHz)
	1	(6, 0 → 5, 0)	2445.811(9)	0
	1	(6, 0 → 5, 0)	2445.811(9)	0
	1	(5, 1 → 4, 1)	2083.853(13)	− 4
	137.163	(5, 1 → 4, 1)	2044.550(15)	6
$^8G_{7/2}$	10	(5, −1 → 5, −2)	14.480(20)	5
	10	(3, 1 → 3, 0)	20.643(20)	− 5
	10	(2, 2 → 2, 1)	31.110(16)	− 10
	20	(5, −1 → 5, −2)	28.963(9)	− 3
	20	(4, 0 → 4, −1)	33.077(15)	− 30
	50	(5, −1 → 5, −2)	72.563(10)	15
	50	(4, 0 → 4, −1)	82.931(20)	− 2
	50	(3, 1 → 3, 0)	102.997(15)	− 15
	100	(5, −1 → 5, −2)	145.555(18)	7
	100	(4, 0 → 4, −1)	166.545(12)	13
	100	(3, 1 → 3, 0)	206.500(15)	− 16
	100	(2, 2 → 2, 1)	319.825(20)	8
	100	(5, −1 → 5, −2)	145.552(22)	4
	100	(4, 0 → 4, −1)	166.500(15)	− 32
	100	(3, 1 → 3, 0)	206.518(14)	2
	100	(2, 2 → 2, 1)	319.808(15)	− 9
	200	(3, 1 → 3, 0)	421.267(25)	− 12
	200	(5, −1 → 5, −2)	293.000(20)	− 3
	200	(4, 0 → 4, −1)	336.577(22)	4
	200	(2, 2 → 2, 1)	648.210(25)	− 9
	400	(5, −1 → 5, −2)	594.403(14)	9
	400	(4, 0 → 4, −1)	692.967(15)	2
	400	(3, 1 → 3, 0)	892.910(20)	2
	1	(5, −1 → 4, −1)	3482.166(12)	0
	1	(4, 0 → 3, 0)	2156.765(12)	0
	1	(3, 1 → 2, 1)	1249.810(12)	− 19
	110	(3, 1 → 2, 1)	1191.680(14)	24
$^8D_{9/2}$	50	(6, −1 → 6, −2)	81.259(18)	19
	100	(6, −1 → 6, −2)	162.990(20)	30
	200	(6, −1 → 6, −2)	328.029(20)	0
	400	(6, −1 → 6, −2)	665.798(20)	− 16
	50	(5, 0 → 5, −1)	92.025(15)	31
	400	(5, 0 → 5, −1)	757.645(25)	12
	400	(4, 1 → 4, 0)	913.779(18)	− 17
	50	(3, 2 → 3, 1)	149.700(15)	14
	100	(3, 2 → 3, 1)	301.147(20)	19
	200	(3, 2 → 3, 1)	605.505(20)	8
	1	(6, −1 → 5, −1)	2756.962(13)	0
	1	(5, 0 → 4, 0)	2175.811(15)	0
	1	(4, 1 → 3, 1)	1660.464(12)	− 4
	122.5	(4, 1 → 3, 1)	1613.820(13)	4
$^8G_{5/2}$	10	(4, −1 → 4, −2)	11.877(6)	13
	20	(4, −1 → 4, −2)	23.763(5)	9
	50	(4, −1 → 4, −2)	59.600(20)	21
	100	(4, −1 → 4, −2)	119.822(10)	5
	200	(4, −1 → 4, −2)	242.318(12)	− 21
	10	(3, 0 → 3, −1)	13.453(10)	2
	20	(3, 0 → 3, −1)	26.945(6)	11
	50	(3, 0 → 3, −1)	67.623(20)	20

TABLE II. *(continued)*

Configuration and state designation	H (G)	Transition $(F, M \rightarrow F', M')$	Observed resonance frequency (MHz)	$\nu^{obs} - \nu^{calc}$ (kHz)
	100	(3, 0 → 3, −1)	136.231(9)	10
	200	(3, 0 → 3, −1)	277.473(12)	− 16
	10	(2, 1 → 2, 0)	17.330(13)	4
	20	(2, 1 → 2, 0)	34.554(15)	13
	100	(2, 1 → 2, 0)	171.393(7)	11
	200	(2, 1 → 2, 0)	355.973(13)	12
	400	(4, −1 → 4, −2)	496.192(14)	− 5
	400	(4, −1 → 4, −2)	496.193(15)	− 4
	400	(2, 1 → 2, 0)	809.600(20)	1
	400	(4, −1 → 4, −2)	496.187(15)	− 10
	400	(3, 0 → 3, −1)	582.498(20)	9
	400	(2, 1 → 2, 0)	809.612(25)	13
	1	(4, −1 → 3, −1)	2826.005(12)	0
	1	(3, 0 → 2, 0)	1837.797(14)	0
	1	(2, 1 → 1, 1)	1089.731(10)	− 7
	1	(2, 2 → 1, 1)	1091.480(11)	5
	155	(2, 1 → 1, 1)	958.780(20)	3
$^8G_{3/2}$	10	(3, −1 → 3, −2)	7.168(10)	10
	20	(3, −1 → 3, −2)	14.348(5)	8
	35	(3, −1 → 3, −2)	25.162(3)	5
	50	(3, −1 → 3, −2)	36.030(7)	4
	100	(3, −1 → 3, −2)	72.635(5)	− 1
	200	(3, −1 → 3, −2)	147.606(4)	− 5
	400	(3, −1 → 3, −2)	304.736(20)	− 12
	20	(2, 0 → 2, −1)	14.388(4)	6
	35	(2, 0 → 2, −1)	25.275(7)	6
	50	(2, 0 → 2, −1)	36.247(10)	2
	100	(2, 0 → 2, −1)	73.477(3)	6
	200	(2, 0 → 2, −1)	151.197(9)	6
	400	(2, 0 → 2, −1)	323.702(20)	− 11
	1	(2, 2 → 1, 1)	1783.600(20)	17
	1	(2, 1 → 1, 0)	1783.600(20)	19
	1	(2, 1 → 1, 1)	1782.862(10)	− 6
	1	(2, 0 → 1, 0)	1782.862(10)	− 4
	1	(2, 0 → 1, 1)	1782.160(20)	6
	1	(3, −1 → 2, −1)	2637.489(10)	− 3
	2	(3, −1 → 2, −1)	2637.505(20)	13
$^8F_{13/2}$	20	(5, 2 → 5, 1)	52.700(25)	− 17
	50	(7, 0 → 7, −1)	95.070(17)	43
	50	(6, 1 → 6, 0)	109.091(16)	35
	50	(5, 2 → 5, 1)	132.015(20)	27
	100	(8, −1 → 8, −2)	171.655(15)	23
	100	(7, 0 → 7, −1)	190.270(20)	17
	100	(6, 1 → 6, 0)	218.190(20)	6
	100	(5, 2 → 5, 1)	264.485(20)	11
	200	(8, −1 → 8, −2)	344.515(12)	− 17
	200	(7, 0 → 7, −1)	381.663(17)	2
	200	(6, 1 → 6, 0)	437.200(20)	− 19
	200	(5, 2 → 5, 1)	529.667(18)	− 23
	400	(8, −1 → 8, −2)	695.260(20)	5
	400	(7, 0 → 7, −1)	770.212(20)	3
	400	(6, 1 → 6, 0)	880.630(20)	3
	400	(5, 2 → 5, 1)	1052.350(30)	0

TABLE II. (continued)

Configuration and state designation	H (G)	Transition $(F, M \longleftrightarrow F', M')$	Observed resonance frequency (MHz)	$\nu^{obs} - \nu^{calc}$ (kHz)
	1	(8, −1 ↔ 7, −1)	2880.387(10)	0
	1	(7, 0 ↔ 6, 0)	2471.480(14)	0
	1	(6, 1 ↔ 5, 1)	2081.816(11)	− 5
	117.395	(6, 1 ↔ 5, 1)	2055.560(15)	9
$^8D_{7/2}$	10	(3, 1 ↔ 3, 0)	22.980(25)	23
	10	(2, 2 ↔ 2, 1)	34.652(25)	33
	20	(3, 1 ↔ 3, 0)	45.892(20)	14
	20	(2, 2 ↔ 2, 1)	69.517(20)	− 2
	50	(3, 1 ↔ 3, 0)	114.637(25)	29
	50	(2, 2 ↔ 2, 1)	175.835(17)	37
	100	(5, −1 ↔ 5, −2)	163.200(20)	12
	100	(4, 0 ↔ 4, −1)	185.970(20)	14
	100	(3, 1 ↔ 3, 0)	230.205(20)	− 11
	100	(2, 2 ↔ 2, 1)	357.026(20)	−2
	200	(5, −1 ↔ 5, −2)	331.710(15)	− 16
	200	(4, 0 ↔ 4, −1)	378.737(15)	5
	200	(3, 1 ↔ 3, 0)	472.129(15)	− 16
	200	(2, 2 ↔ 2, 1)	719.607(17)	11
	400	(3, 1 ↔ 3, 0)	996.270(35)	− 4
	1	(5, −1 ↔ 4, −1)	1694.560(10)	0
	1	(4, 0 ↔ 3, 0)	1475.932(13)	0
	1	(3, 1 ↔ 2, 1)	1176.205(20)	− 10
	110	(3, 1 ↔ 2, 1)	1112.637(15)	6
$^8G_{1/2}$	1	(2, 1 ↔ 2, 2)	0.427(7)	8
	10	(2, 1 ↔ 2, 2)	4.195(10)	3
	50	(2, 1 ↔ 2, 2)	21.169(6)	3
	100	(2, 1 ↔ 2, 2)	42.849(7)	2
	200	(2, 1 ↔ 2, 2)	87.797(4)	− 1
	400	(2, 1 ↔ 2, 2)	184.430(15)	1
	900	(2, 1 ↔ 2, 2)	469.720(20)	0
$^8H_{17/2}$	10	(8, 1 ↔ 8, 0)	20.405(30)	39
	10	(7, 2 ↔ 7, 1)	23.400(15)	19
	20	(8, 1 ↔ 8, 0)	40.750(30)	19
	20	(7, 2 ↔ 7, 1)	46.770(30)	− 4
	50	(9, 0 ↔ 9, −1)	91.353(13)	26
	50	(8, 1 ↔ 8, 0)	101.840(15)	14
	50	(7, 2 ↔ 7, 1)	117.017(15)	6
	100	(10, −1 ↔ 10, −2)	167.453(11)	25
	100	(9, 0 ↔ 9, −1)	182.740(12)	23
	100	(8, 1 ↔ 8, 0)	203.720(10)	31
	100	(7, 2 ↔ 7, 1)	234.220(11)	6
	200	(9, 0 ↔ 9, −1)	365.810(25)	13
	200	(8, 1 ↔ 8, 0)	407.830(20)	9
	200	(7, 2 ↔ 7, 1)	468.760(15)	28
	400	(10, −1 ↔ 10, −2)	671.815(25)	6
	400	(9, 0 ↔ 9, −1)	733.833(25)	2
	400	(8, 1 ↔ 8, 0)	819.340(25)	33
	400	(7, 2 ↔ 7, 1)	935.050(25)	− 7
	800	(10, −1 ↔ 10, −2)	1351.130(40)	− 44
	800	(9, 0 ↔ 9, −1)	1481.560(50)	− 68
	800	(8, 1 ↔ 8, 0)	1656.595(50)	− 106
	800	(7, 2 ↔ 7, 1)	1842.070(45)	− 61
	1	(8, 1 ↔ 7, 1)	2532.402(10)	0
	1	(9, 0 ↔ 8, 0)	4112.643(15)	0

TABLE II. (continued)

Configuration and state designation	H (G)	Transition $(F, M \longleftrightarrow F', M')$	Observed resonance frequency (MHz)	$\nu^{obs} - \nu^{calc}$ (kHz)
$^8D_{5/2}$	1	(10, −1 ↔ 9, −1)	6138.846(12)	0
	5	(2, 1 ↔ 2, 0)	11.710(30)	− 2
	10	(2, 1 ↔ 2, 0)	23.395(25)	31
	20	(4, −1 ↔ 4, −2)	32.550(30)	21
	20	(3, 0 ↔ 3, −1)	36.528(25)	45
	20	(2, 1 ↔ 2, 0)	46.540(20)	5
	50	(2, 1 ↔ 2, 0)	116.187(20)	30
	100	(4, −1 ↔ 4, −2)	173.200(15)	− 2
	100	(3, 0 ↔ 3, −1)	187.680(18)	− 6
	100	(2, 1 ↔ 2, 0)	240.590(15)	− 9
	200	(3, 0 ↔ 3, −1)	397.203(25)	− 14
	200	(2, 1 ↔ 2, 0)	539.873(25)	9
	1	(4, −1 ↔ 3, −1)	541.780(20)	0
	1.186	(3, 0 ↔ 2, 0)	827.785(13)	0
	0.500	(2, 1 ↔ 1, 1)	751.645(15)	− 45
	1	(2, 1 ↔ 1, 1)	750.635(22)	8
	1.800	(2, 1 ↔ 1, 1)	748.955(17)	21
$4f^85d6s^2$? $^8H_{15/2}$?	1	(9, −1 ↔ 8, −1)?	5171.397(10)	3
	2	(9, −1 ↔ 8, −1)?	5171.550(11)	− 4

served[1] value of g_J. It is certainly not identified, as such, however, and could well belong to another state.

An unusual feature of the experiment was the observation of the strongly negative g_J value for the $^8G_{1/2}$ state. The result was expected, however, on the basis of the optical measurements[1] (as well as from the Landé formula), and no particular experimental difficulty was encountered.

IV. THEORETICAL ANALYSIS

A. Classification of States

Tb is the only neutral atom, except for some transuranics, whose atomic ground state is not yet known[18] with certainty. Bender, Penselin, and Schlupmann[2] concluded that the $4f^85d6s^2$ $^8G_{15/2}$ and $4f^96s^2$ $^6H_{15/2}$ states are separated by not more than 1000 cm⁻¹, and that the atomic ground state is $4f^85d6s^2$ $^8G_{15/2}$. Meinders and Klinkenberg[1] have since shown, however, that in the $4f^85d6s^2$ configuration, $^8G_{13/2}$ lies 176.580 cm⁻¹ below $^8G_{15/2}$.

The problem of determining the ground state is as difficult as it is important. Since the two configurations f^8ds^2 and f^9s^2 have opposite parity, optical studies lead to two unrelated systems. While levels of both configurations are populated in an atomic beam of Tb, the only way of estimating relative excitation energies (unless selective excitation is used) is to try to determine the Boltzmann factors by studying relative intensities of rf tran-

sitions. It has been pointed out above that the ob-
served intensity depends strongly on several fac-
tors, especially on the intensity and distribution
of the rf magnetic field in the particular region of
the homogeneous magnetic field (C field) in which
the transition is induced. Some effort was made
in the course of the present work to compare the
relative intensities of transitions in $4f\,^9 6s^2\,{}^6 H_{15/2}$,
$4f\,^8 5d 6s^2\,{}^8 G_{15/2,\,13/2,\,11/2}$ at a variety of rf power
levels and for each possible value of F. Lack of
self-consistency in the data ruled out a conclusive
result, unfortunately.

The series of papers of Meinders and Klinken-
berg[1] on the classification of levels of the $4f\,^8 5d 6s^2$
configuration of Tb I was of the very greatest im-
portance for the present experiment. Through
their optical work, they assigned the relative ex-
citation energy, the J value, and the g_J value to
all $4f\,^8 5d 6s^2$ levels through about 8700 cm^{-1}.

B. Development of Eigenvectors

Arnoult and Gerstenkorn,[3] in addition to making
optical studies of the hfs of the $4f\,^8 5d 6s^2$
$^8 G_{15/2,\,13/2,\,11/2}$ states, made a computer fit to all
the known levels of the configuration, and thereby
obtained eigenvectors for each state. In setting
up the problem, they recognized that the configura-
tion would have to be very severely truncated
(119 LS terms arise[19] from the $f\,^8$ core). They
felt that, as a first approximation for the low-
lying levels, it would be reasonable to restrict the
$f\,^8$ core to the single $^7 F$ term since it could be ex-
pected to lie considerably below all others. Even
this drastic cutoff leads to both octets and sextets
with $L = 1, 2, 3, 4,$ and 5 when the single d electron
is added. (The higher-lying $4f\,^8 5d^2 6s$ configuration
was ignored.) They found that except for very
large and very small J, virtually all states are
far removed from the LS limit. As an example,
the leading terms in the (SL) eigenvector for the
1085-cm^{-1} level designated $^8 G_{9/2}$ were found to be

$$\left|\,^8 G_{9/2}'\right\rangle = 0.582\left|\,^8 G\right\rangle + 0.579\left|\,^8 F\right\rangle$$
$$+ 0.523\left|\,^8 D\right\rangle + 0.179\left|\,^8 P\right\rangle + \cdots . \quad (4)$$

Although assignment of quantum numbers S and L
to such states is physically meaningless, it is
nevertheless convenient for discussion, and the
labels or designations of Meinders and Klinken-
berg[1] (Table I) are used throughout this paper.
It has been pointed out[10] that these eigenvectors,
derived from computer fits to the optically de-
termined energies, are remarkably satisfactory
in accounting for the magnetic-dipole hyperfine-
interaction constants for the low-lying states.
Comparison of the experimental and calculated
values of the electric-quadrupole hfs constants

B, however, showed that it was desirable to try
to improve the eigenvectors. As a first step,
Crosswhite[20] extended the permissible terms of
the $f\,^8$ core to include the five quintets which (a)
can mix directly with $^7 F$ by the spin-orbit inter-
action, and (b) lie sufficiently low to be potentially
important, namely, all three $^5 D$ terms and those
labeled $^5 G_1$ and $^5 G_3$ by Nielson and Koster,[19] in
addition to the $^7 F$ term already included. The
eigenvectors found showed that for all of the levels
of Table I, 96% or more of the strength arises
from the $^7 F$ core term. The Crosswhite eigen-
vectors fit the term values, g_J values, and hyper-
fine-interaction constants slightly better than do
the Arnoult-Gerstenkorn[3] eigenvectors. Even
though the improvement in fits is slight, it is
hoped that the hfs parameters found with Cross-
white's eigenvectors are more meaningful phys-
ically since the $f\,^8$ core is allowed more freedom.

The relative excitation energies, g_J values,
and eigenvectors of the $4f\,^9 6s^2\,{}^6 H_{15/2,\,13/2,\,11/2}$
states were calculated by Conway and Wybourne.[4]
All three were found to be at least 94% pure, in
marked contrast to the states of $4f\,^8 5d 6s^2$.

C. Values of the Electron g Factors

The Conway-Wybourne calculated intermedi-
ate-coupling g_J values for the $4f\,^9 6s^2\,{}^6 H$ levels
were corrected for relativistic and diamagnetic
effects only in the case of the $^6 H_{15/2}$ state, since
this was the only state of the configuration for
which an experimental g_J value was currently
available. The calculated value lies only 0.08%
below the observed.

Judd and Lindgren[5] have also calculated the g_J
values of these states. Their calculated values
are smaller than the observed by 0.1–0.6%. The
calculation cannot be made with high precision,
especially, for the excited states, without knowl-
edge of the relative spacings of the levels.

Of the fourteen $4f\,^8 5d 6s^2$ levels for which precise
g_J values were obtained, in 13 states the values
calculated from Crosswhite's eigenvectors[20] dif-
fer from observation by 1.7% or less. (While this
difference may seem small, it is typically 500
times the experimental standard deviation.) For
the 14th state $^8 G_{1/2}$ the difference is 3.1% even
though the state is about the purest (94%) consid-
ered. The reason is that the Landé value of g_J
$(^8 G_{1/2}) = -\frac{4}{3}$ is drastically altered by even minute
admixtures of states with more normal (i.e., pos-
itive), values of g_J.

D. Hamiltonian for the Hyperfine Interaction

It has been pointed out above that generalization
of the expression given in Eq. (2) for $\mathcal{H}_{\text{hfs}}$ is es-

sential. In general, the hyperfine interaction can be represented[21] as a sum of scalar products of tensor operators

$$\mathcal{H}_{hfs} = \sum_k \vec{T}_n^{(k)} \cdot \vec{T}_e^{(k)} \ , \qquad (5)$$

where n and e refer to the nucleus and to the electrons, respectively, and k is the rank of the tensor operator involved. If we limit ourselves to the magnetic-dipole, electric-quadrupole, and magnetic-octupole interactions, we have $k = 1, 2,$ and 3 only. Sandars and Beck have shown[21] that only three tensor operators may contribute to the electronic part for each k: $\vec{U}^{(0,k)k}$, $\vec{U}^{(1,k-1)k}$, and $\vec{U}^{(1,k+1)k}$, where the $\vec{U}^{(k_s, k_l)k}$ are double tensor operators, described by Judd,[22] with rank $k_s, k_l,$ and k in spin, orbital, and combined space, respectively. For the magnetic-dipole case, the required operators $\vec{U}^{(01)1}$, $\vec{U}^{(10)1}$, and $\vec{U}^{(12)1}$ are proportional to

$$\vec{L} = \sum \vec{l}_i, \quad \vec{S} = \sum \vec{s}_i, \qquad \sum [\vec{s} \times \vec{C}^{(2)}]_i^{(1)} \ ,$$

respectively, where $\vec{C}^{(2)}$ is itself proportional to the spherical harmonic of order 2. The relative contribution of each of these terms is here regarded as being determined by an adjustable parameter $a_l^{k_s, k_l}$. Thus, for the magnetic-dipole hyperfine interaction, in configurations of the types l^N or $l^N l'$, we may write

$$\mathcal{H}_{hfs}(M1) = \sum_{i=1}^N [a_l^{01} \vec{l}_i - 10^{1/2} a_l^{12} (\vec{s} \times \vec{C}^{(2)})_i^{(1)} + a_l^{10} \vec{s}_i] \cdot \vec{I}$$

$$+ [a_{l'}^{01} \vec{l}_{N+1} - 10^{1/2} a_{l'}^{12} (\vec{s} \times \vec{C}^{(2)})_{N+1}^{(1)} + a_{l'}^{10} \vec{s}_{N+1}] \cdot \vec{I} \ , \qquad (6)$$

where the term applying to the $(N+1)$th electron is dropped if we restrict ourselves to the l^N configuration. The factor of $10^{1/2}$ is conventional, and only a matter of definition. In the nonrelativistic limit and in the absence of configuration interaction, it can be shown that $a_l^{01} = a_l^{12} = a_{nl} \equiv 2\mu_B \mu_N \times (\mu_I/I)\langle r^{-3}\rangle_{nl}$ and that for $l, l' \neq 0$, we have $a_l^{10} = 0$, and similarly for l'. Sandars and Beck[21] have shown how to calculate the effect of relativity on the $a_l^{k_s, k_l}$ [see Eq. (A12)], but the effects of configuration interaction are often more severe and far less susceptible to calculation.

For the electric-quadrupole hyperfine interaction, the Hamiltonian for the configuration l^N or $l^N l'$ may be written

$$\mathcal{H}_{hfs}(E2) = \frac{r_n^2}{Q} \vec{C}_n^{(2)} \cdot \left\{ \sum_{i=1}^N \left[b_l^{02} \left(\frac{2l(l+1)(2l+1)}{(2l-1)(2l+3)} \right)^{1/2} \right. \right.$$

$$\left. \times \vec{U}_i^{(02)2} + (\tfrac{3}{10})^{1/2} b_l^{13} \vec{U}_i^{(13)2} + (\tfrac{3}{10})^{1/2} b_l^{11} \vec{U}_i^{(11)2} \right]$$

$$+ \left[b_{l'}^{02} \left(\frac{2l'(l'+1)(2l'+1)}{(2l'-1)(2l'+3)} \right)^{1/2} \vec{U}_{N+1}^{(02)2} \right.$$

$$+ (\tfrac{3}{10})^{1/2} b_{l'}^{13} \vec{U}_{N+1}^{(13)2} + (\tfrac{3}{10})^{1/2} b_{l'}^{11} \vec{U}_{N+1}^{(11)2} \right] \right\} \ , \qquad (7)$$

where $er_n^2 \vec{C}_n^{(2)} = \vec{T}_n^{(2)}$ $\qquad (8)$

and $\langle II | T_n^{(2)} | II \rangle = \tfrac{1}{2} eQ$. $\qquad (9)$

Again, the term for the $(N+1)$st electron is dropped if we limit our attention to configurations of the type l^N. In these expressions, μ_B and μ_N are the Bohr and nuclear magnetons, μ_I is the nuclear magnetic-dipole moment, and Q is the nuclear electric-quadrupole moment. Nonrelativistically, b^{13} and b^{11} are zero for both l and l', and the quantities b_l^{02} and $b_{l'}^{02}$ approach the nonrelativistic parameters

$$b_{nl} \equiv e^2 Q \langle r^{-3} \rangle_{nl}$$

and $b_{n'l'} \equiv e^2 Q \langle r^{-3} \rangle_{n'l'}$.

The $b_l^{k_s, k_l}$ may be either regarded as independent parameters or calculated by the method of Sandars and Beck[21] if the necessary relativistic radial wave functions are known. Childs and Goodman[23] give expressions which show how these quantities may be numerically related to b_{nl} and $b_{n'l'}$ by the use of the Casimir factors.[24]

The magnetic-octupole term $(k = 3)$ of Eq. (5) can be worked out in similar fashion; but since the present experiment revealed no values of C that are definitely nonzero, and since matrix elements of $\mathcal{H}_{hfs}(M3)$ between different atomic states are vanishingly small, we limit ourselves to the diagonal term, i.e., to the final term of Eq. (2).

E. Parametrized Theoretical Expressions for the Hyperfine Interaction Constants

If the matrix elements of Eqs. (6) and (7) are evaluated between any two states of the same J, the first two terms of Eq. (2) are recovered and, in addition, expressions for the generalized A and B factors between the two states may be deduced in terms of the parameters $a_l^{k_s, k_l}, a_{l'}^{k_s, k_l}, b_l^{k_s, k_l}$, and $b_{l'}^{k_s, k_l}$. The SL basis is most convenient for the calculation. The results are given in the Appendix. With these expressions and the SL eigenvectors of the atomic states, similar expressions can be obtained for the real states of the atom. Such calculations were carried out on digital computers by use of Crosswhite's eigenvectors.[20] The programs were written by Goodman. A typical result is

$$B(4f^8 5d 6s^2 \ {}^8G'_{11/2}) = (0.589\,393\,b_f^{02} + 0.030\,602\,b_f^{13}$$

$$- 0.074\,201\,b_f^{11})$$

$$+(-0.341\,185\,b_d^{02} - 0.071\,437\,b_d^{13}$$

$$+0.021\,206\,b_d^{11})\,,\tag{10}$$

where the prime denotes the real state (in intermediate coupling) of the atom. For comparison, the B factor of the same state in the LS limit (or, more precisely, of the SL basis state of the same name) is entirely different, namely,

$$B(4f^8 5d6s^2\ ^8G_{11/2}) = (0.142\,857\,b_f^{02} - 0.008\,191\,b_f^{13}$$

$$-0.076\,836\,b_f^{11}) + (0.020\,408\,b_d^{02}$$

$$-0.025\,379\,b_d^{13} + 0.069\,231\,b_d^{11})\,.\tag{11}$$

The extent of the departure of this state (and it is typical of many) from its composition in the LS limit should again be emphasized. The largest contribution to the B value of $^8G'_{11/2}$ is the term in b_f^{02}. Not only is this term much larger than that in $^8G_{11/2}$, but it is larger than the corresponding term in all the principal admixtures of $^8G'_{11/2}$; it arises mostly from matrix elements of $\mathcal{K}_{hfs}$ ($E2$) *between* basis states of $^8G'_{11/2}$.

As mentioned in Sec. III D, Sandars and Beck[21] have shown how, if configuration interaction is ignored, the relationship between the quantities $a_l^{ks,kl}$ and a_{nl} may be evaluated by taking the proper combinations of several relativistic radial integrals If these integrals are not available, they may be approximated [as seen in Eqs. (A12)] by the Casimir factors.[24] In the electric-quadrupole hyperfine interaction, the appropriate Casimir factors may similarly be used [as in obtaining Eq. (15) of Ref. 1] to evaluate the quantities $b_l^{ks,kl}$ in terms of b_{nl}. If the appropriate Casimir correction factors are calculated according to the method summarized by Kopfermann,[24] with

$$Z_{eff}(4f) = Z - 35 = 30\,,$$

$$Z_{eff}(5d) = Z - 12 = 53\,,$$

it is found that

$$a_f^{01} = 1.0063\,a_{4f}, \qquad a_d^{01} = 1.0428\,a_{5d}\,,$$

$$a_f^{12} = 1.0157\,a_{4f}, \qquad a_d^{12} = 1.1074\,a_{5d}\,,$$

$$a_f^{10} = -0.0031\,a_{4f}, \qquad a_d^{10} = -0.0209\,a_{5d}\,;$$

$$b_f^{02} = 1.0124\,b_{4f}, \qquad b_d^{02} = 1.0850\,b_{5d}\,,\tag{12}$$

$$b_f^{13} = 0.0356\,b_{4f}, \qquad b_d^{13} = 0.3359\,b_{5d}\,,$$

$$b_f^{11} = -0.0066\,b_{4f}, \qquad b_d^{11} = -0.0572\,b_{5d}\,.$$

If these approximations are used in Eq. (10), it is found that

$$B(4f^8 5d6s^2\ ^8G'_{11/2}) = 0.598\,281\,b_{4f} - 0.395\,399\,b_{5d}\,.\tag{13}$$

The usefulness of this result depends on the accu-

racy of the Casimir factors used. The corresponding expression for the dipole hfs constant A also ignores the distortions of Eq. (12) by configuration interaction. Comparing Eq. (13) with Eq. (10) confirms that most of the quadrupole interaction is associated with the operators $\vec{U}_f^{(02)2}$ and $\vec{U}_d^{(02)2}$, which are the only operators present in the nonrelativistic limit.

F. Corrections for the Effects of hfs and Zeeman Interactions with Other Atomic States

The "uncorrected values" of (and uncertainties in) the hfs constants A, B, and C and of the electron g factor g_J in Table III are the values deduced from the eigenvalue differences obtained from Eqs. (1)–(3) by computer fitting them to observed transition frequencies. The procedure for obtaining these values fails to allow for perturbations of the hyperfine levels (and the resulting shifts in transition frequencies) by hfs and Zeeman interactions with other nearby atomic states. If the perturbing state has the same J as the state in question, Eqs. (1)–(3) will still be capable of fitting the observed hfs spectrum, but the values obtained for the parameters being varied (A, B, C, and g_J) may be altered. Since theoretical predictions of the hfs constants are based on eigenvectors[20] deduced without regard to this type of effect, they may not be directly compared with the experimental values until the latter are corrected for these perturbations. If the J of the perturbing state is different from that of the state in question, then in addition to yielding distorted parameter values, Eqs. (1)–(3) may fail to fit the observed resonance frequencies satisfactorily. This was observed most markedly for the $4f^8 5d6s^2\ ^8G_{3/2,\,5/2}$ states, for which the values of χ^2 fell from 394 and 80, respectively, before correction, to 11 and 15 after.

Several authors[25] have treated this problem for the case in which the atom is near the LS limit and for which the perturbing states have the same S and L as the state in question. Both of these simplifications are grossly inappropriate for Tb, and a more general approach is required. Since the hyperfine and Zeeman perturbations are normally on the order of 10^{-3} of the energy separation of the perturbing states, second-order perturbation theory should give an accurate result. If the state for which energy shifts are required is called Ψ and possible perturbing states are denoted by Ψ', then it can be shown[26] that the energy of a particular magnetic substate of Ψ at field H is shifted by

$$\delta E(\Psi, I\mathcal{F}M) \approx \sum_{\Psi \neq \Psi'} \sum_{F'} \frac{|\langle \Psi, I\mathcal{F}M | \mathcal{K} | \Psi', IF'M \rangle|^2}{E(\Psi) - E(\Psi')}\,,\tag{14}$$

TABLE III. Values of the hyperfine-interaction constants A, B, and C, and of the electron g factor g_J found for the various levels of Tb^{159}. The "uncorrected" value in each case is for a fit to the data on the assumption that the atomic state is perfectly isolated. The "final" value (next to last column) is the value obtained after correcting for the effects of hyperfine and Zeeman perturbations from other atomic states. The χ^2 value for this fit is given at the right. The uncertainties listed with the uncorrected values are simply the output of the computer fitting program and result from uncertainties in observed resonance frequencies. Those listed with the final values are an estimate of the total over-all uncertainty, including uncertainties in the corrections applied.

Configuration	State	Quantity	Uncorrected value and uncertainty (MHz)	Final value and total uncertainty assigned (MHz)	χ^2
$4f^9 6s^2$	$^6H_{15/2}$	A	673.755(1)	673.753(2)	7
		B	1449.445(12)	1449.330(40)	
		C	0.001(1)	−0.001(2)	
		g_J	1.32514(1)	1.32513(2)	
	$^6H_{13/2}$	A	682.922(1)	682.911(3)	15
		B	1167.710(19)	1167.489(50)	
		C	0.001(1)	−0.001(2)	
		g_J	1.27625(1)	1.27625(2)	
	$^6H_{11/2}$	A	730.4±1.3	729.9±2.0	20
		B	986.7±12	982.9±15	
		g_J	1.20610(2)	1.20610(3)	
$4f^8 5d6s^2$	$^8G_{13/2}$	A	532.206(1)	532.204(2)	2
		B	928.978(10)	928.861(30)	
		C	0.003(1)	0.001(2)	
		g_J	1.46449(2)	1.46448(2)	
	$^8G_{15/2}$	A	472.646(1)	472.643(2)	14
		B	1154.271(11)	1154.239(17)	
		C	−0.003(1)	0.001(2)	
		g_J	1.45624(2)	1.45624(2)	
	$^8G_{11/2}$	A	577.472(1)	577.465(2)	11
		B	990.046(10)	989.917(30)	
		C	−0.001(1)	−0.002(2)	
		g_J	1.51654(2)	1.51654(3)	
	$^8G_{9/2}$	A	602.232(1)	602.219(3)	12
		B	1267.402(11)	1267.267(30)	
		C	0.003(1)	0.001(2)	
		g_J	1.54110(2)	1.54110(2)	
	$^8D_{11/2}$	A	405.118(1)	405.106(3)	10
		B	−92.432(13)	−92.638(50)	
		C	0.002(1)	0.001(2)	
		g_J	1.53021(2)	1.53020(2)	
	$^8G_{7/2}$	A	591.596(2)	591.564(7)	17
		B	733.550(11)	733.233(70)	
		C	0.003(1)	−0.001(2)	
		g_J	1.47680(2)	1.47678(2)	
	$^8D_{9/2}$	A	441.792(2)	441.771(5)	9
		B	158.966(12)	158.750(40)	
		C	0.003(1)	0.000(2)	
		g_J	1.54375(2)	1.54375(3)	
	$^8G_{5/2}$	A	652.838(2)	652.766(20)	15
		B	268.077(9)	267.611(150)	
		C	0.005(1)	0.001(2)	
		g_J	1.35528(2)	1.35525(3)	

TABLE III. (*continued*)

Configuration	State	Quantity	Uncorrected value and uncertainty (MHz)	Final value and total uncertainty assigned (MHz)	χ^2
	$^8G_{3/2}$	A	884.072(2)	883.905(30)	11
		B	−14.723(5)	−15.510(250)	
		g_J	1.02225(2)	1.02220(4)	
	$^8F_{13/2}$	A	354.461(1)	354.454(3)	16
		B	72.320(11)	72.183(30)	
		C	0.001(1)	0.000(2)	
		g_J	1.50473(2)	1.50473(3)	
	$^8D_{7/2}$	A	358.951(2)	358.918(7)	9
		B	−140.630(11)	−140.881(50)	
		C	0.004(1)	0.002(2)	
		g_J	1.64185(3)	1.64184(3)	
	$^8G_{1/2}$	A	2595.3±1.1	2584.8±4.0	2
		g_J	−1.19306(7)	−1.19125(30)	
	$^8H_{17/2}$	A	481.740(1)	481.738(2)	28
		B	2246.145(13)	2245.914(50)	
		C	0.007(1)	0.001(2)	
		g_J	1.40626(2)	1.40626(4)	
	$^8D_{5/2}$	A	215.706(3)	215.653(15)	11
		B	−401.604(14)	−401.862(60)	
		C	0.003(1)	0.001(2)	
		g_J	1.83132(5)	1.83129(7)	

where the script $\mathcal{F}$ indicates the particular linear combination of F's that, in the absence of the perturbing interaction $\mathcal{H}$, characterize the substate at field H. In most cases, the LS-limit representation of the states Ψ and Ψ' with angular momenta J and J', respectively, may be used in Eq. (14). For states as far removed from the LS limit as the $4f^8 5d6s^2$ levels of Tb, however, it is essential to use the complete LS eigenvectors for the states Ψ and Ψ'. Although the expression (14) for the shift appears simple, it contains four coherent sums; one each over the eigenvector components of Ψ and Ψ', one over the F composition of Ψ, and one over the various hfs and Zeeman operators that appear in $\mathcal{H}$. Thus in calculating frequency shifts for five transitions at three values of H in one state Ψ, for example, something like 30 000-50 000 matrix elements of $\mathcal{H}$ must be calculated. While somewhat more than half of these will typically vanish, evaluation of each element that does not vanish requires calculation of 10-20 nonzero 3-, 6-, and 9-j symbols. Such a calculation is carried out in a few minutes on the IBM-360-75. Table IV illustrates the results of the calculation for two transitions in the $^8G_{3/2}$ state; all states (a) whose J differed from $\frac{3}{2}$ by 2 or less and (b) whose excitations were less than 6000 cm^{-1} were considered. The shifts are seen to be large compared with the typical experimental uncertainty of 0.010 MHz. Most of the shift comes, as expected, from the

TABLE IV. Frequency shifts calculated from Eq. (14) for two transitions in the $^8G_{3/2}$ state. The contributions to the shift caused by hfs and Zeeman interactions with seven nearby atomic states are listed separately. The intermediate-coupling eigenvectors of both the perturbed and perturbing states are used explicitly in the calculation.

Perturbing state	Excitation energy of perturbing state (cm^{-1})	Change in resonance frequency (MHz)	
		$F = 3 \leftrightarrow F = 2$ $H = 0$	$(2, 0 \leftrightarrow 2, -1)$ $H = 400$ G
$^8G_{7/2}$	2134	0.0007	0.0000
$^8G_{5/2}$	2889	0.2266	−0.0940
$^8D_{7/2}$	3534	0.0000	0.0000
$^8G_{1/2}$	3733	1.0561	0.3091
$^8D_{5/2}$	4410	0.0026	0.0018
$^8D_{3/2}$	5199	0.0007	0.0004
$^8F_{1/2}$	5974	0.0000	0.0000
	Total shift	+1.287	+0.217

states $^8G_{5/2}$ and $^8G_{1/2}$. The eigenvectors of Arnoult and Gerstenkorn[3] were used for calculating all of the corrections applied.

The interaction $\mathcal{K}$ of Eq. (14) is taken to consist of the magnetic-dipole and electric-quadrupole hyperfine-interaction operators given by Eqs. (6) and (7) plus the generalized Zeeman operator $\mathcal{K}_z$ given by Eq. (A9) of the Appendix. In the computer program for evaluation of the shifts represented by Eq. (14), the quadrupole operator is restricted to be nonrelativistic, i.e., the coefficients of the operators $\vec{U}^{(13)2}$ and $\vec{U}^{(11)2}$ are taken to be zero. This simplification is reasonable for the two configurations considered in Tb, and should be excellent for the part due to $4f$ electrons. The operator $\vec{U}^{(13)2}$ can make an important contribution in the $5d$ shell, but the effect on the shifts calculated by Eq. (14) is diluted by the larger contribution of the $4f$ electrons, and by the magnetic-dipole element as well.

It should be emphasized that in deriving Eq. (14) for the shifts, the effect treated as a small perturbation is the switching on of hfs and Zeeman interactions between the state Ψ and other nearby states Ψ'; the departure of the atom from the LS and the presence of the magnetic field, for example, are not treated as perturbations. Comparison of the predictions of Eq. (14) with a calculation that diagonalizes the complete matrix of all J and F at arbitrary H showed excellent agreement for the case of a single LS multiplet in the LS limit. Both computer programs were written by Goodman at Argonne.

In Table III, the "final" values of the hfs constants A, B, and C, of the electron g factor g_J, and of χ^2 are the values obtained by computer fits of the theoretical transition frequencies [obtained

with Eqs. (1)–(3) and (14)] to the experimental. Corrections to the A values are much larger than experimental error in most cases, but are less than 0.1% for all states except $^8G_{1/2}$ for which the zero-field hfs interval has not yet been observed. The correction to B, though larger absolutely, is still small except for $^8G_{3/2}$ for which it is 5%. The correction to the magnetic-octupole hfs interaction constant exceeds 100% for some states and has the effect of reducing the occasionally large apparent values of C. After making the corrections and allowing for the associated uncertainties, the value of C is zero to within the quoted uncertainty for every state. Corrections to the g_J values are very small for all states except $^8G_{1/2}$. Because of the large effect in this state, the corrections to the calculated transition frequencies for $^8G_{1/2}$ were recomputed with Crosswhite's eigenvectors.[20] The corrected value of A was virtually unchanged, while the shift in g_J (from the uncorrected value) was only 7% different from that calculated with Arnoult and Gerstenkorn's eigenvectors.[3] The uncertainty given is large enough to include this difference.

G. Algebraic Signs of the Hyperfine Interaction Constants A, B, and C

In the present experiment, only the sign of B/A (and with less certainty of C/A) is measured, and the algebraic sign of A for each state must be inferred from theoretical considerations. The algebraic signs of μ_1 and Q for Tb^{159} are both known[8] to be positive, however, and consequently the quantities

$$a_{nl} \equiv 2\mu_B\mu_N(\mu_I/I)\langle r^{-3}\rangle_{nl}$$

$$\text{and} \quad b_{nl} \equiv e^2Q\langle r^{-3}\rangle_{nl} \tag{15}$$

are both positive for each shell nl. It has been shown above how theoretical expressions for the A's and B's of the 17 states investigated in Tb^{159} may be derived in terms of the parameters $a_l^{k_s, k_l}$ and $b_l^{k_s, k_l}$, and how these in turn may be related (if configuration interaction is ignored) to a_{nl} and b_{nl} by use of the appropriate Casimir factors. When this is done, it is found that both A and B must be positive for $4f^96s^2$ $^6H_{15/2, 13/2, 11/2}$. It is also found that the largest part of A (that due to the $4f$ electrons) is positive for all of the states examined in $4f^85d6s^2$, and that for reasonable values of a_{5d}, A must be positive for all the states examined. Chan and Unsworth[6] have confirmed this experimentally for the $^8G_{15/2, 13/2, 11/2}$ states of $4f^85d6s^2$. Strong theoretical arguments, based on similar considerations, can be made to support the signs reported for all the B values, but since these signs follow from the positive sign of A and the measured signs of B/A, the theoretical arguments are unnecessary.

H. Fitting the Parametrized Theoretical Expressions for A and B to the Measured Values

In Secs. IV F–IV G, it has been shown how experimental values of the hyperfine-interaction constants are deduced from the observed transition frequencies, how these values are corrected for the effects of hyperfine and Zeeman interactions with other states, and how algebraic signs are assigned to the measured magnitudes. It has also been shown how theoretical expressions are developed for each of these hyperfine-interaction constants. The expressions are in terms of the quantities $a_l^{k s, k l}$ and $b_l^{k s, k l}$, which may be regarded as adjustable parameters. Alternatively, if configuration interaction is believed to play a small role, and if the Casimir correction factors are trusted, the quantities $a_l^{k s, k l}$ and $b_l^{k s, k l}$ may be expressed in terms of the nonrelativistic radial integrals a_{nl} and b_{nl} by Eq. (12). Thus, for the $4f^9 6s^2$ configuration, the A factors for each state may be expressed either in terms of the three quantities $a_f^{01}, a_f^{12}, a_f^{10}$ or the single parameter a_{4f}, and the B factors in terms of $b_f^{02}, b_f^{13}, b_f^{11}$ or just b_{4f}. For the $4f^8 5d 6s^2$ configuration, which contains an unfilled $5d$ shell as well as the $4f$ shell, corresponding terms must be included to describe the dependence of the hyperfine constants on the $5d$ electron. It should also be noted that the parameters referring to the $4f$ shell may have slightly different values in the two configurations.

When the three measured A or B values in the $4f^9 6s^2$ configuration ($^6H_{15/2,\,13/2,\,11/2}$) are fitted with the 3-parameter expressions, perfect fits of course result. The fits obtained by using only one parameter (a_{4f} or b_{4f}) are shown in Table V. Although the fits appear good, they are in reality little better than those obtained in the LS limit. Discussion of the fits, and of the parameter values obtained, will be deferred to Sec. IV J.

TABLE V. Results of 3- and 1-parameter fits to the dipole and quadrupole hfs constants of three ^6H states of $4f^9 6s^2$ in Tb[159]. Both fits explicitly include all three types of permissible tensor interactions. The relative amounts of each are determined by free parameters in the 3-parameter fits, but assumed to be given by the appropriate relativistic correction factors in the 1-parameter fits. The 3-parameter fits are, of course, perfect.

Configuration and state	3-parameter fits		1-parameter fits	
	$A^{obs}-A^{calc}$ (%)	$B^{obs}-B^{calc}$ (%)	$A^{obs}-A^{calc}$ (%)	$B^{obs}-B^{calc}$ (%)
$4f^9 6s^2\,{}^6H_{15/2}$	0	0	0.4	4
$4f^9 6s^2\,{}^6H_{13/2}$	0	0	-0.5	-2
$4f^9 6s^2\,{}^6H_{11/2}$	0	0	0.1	-2

TABLE VI. Results of 6- and 2-parameter fits to the dipole and quadrupole hfs constants of 14 states of $4f^8 5d 6s^2$ in Tb[159]. Both fits allow all three possible types of tensor interactions for each of the two unfilled electron shells, $4f$ and $5d$. The 6-parameter fits allow the relative amounts of each interaction to be determined by a free parameter; the relative amounts are assumed to be given by the appropriate relativistic correction factors for the 2-parameter fits.

Configuration and state	6-parameter fits		2-parameter fits	
	$A^{obs}-A^{calc}$ (%)	$B^{obs}-B^{calc}$ (%)	$A^{obs}-A^{calc}$ (%)	$B^{obs}-B^{calc}$ (%)
$4f^8 5d 6s^2\,{}^8G_{13/2}$	1	-1	-1	11
$4f^8 5d 6s^2\,{}^8G_{15/2}$	0	-2	-1	9
$4f^8 5d 6s^2\,{}^8G_{11/2}$	0	1	1	14
$4f^8 5d 6s^2\,{}^8G_{9/2}$	-1	7	3	6
$4f^8 5d 6s^2\,{}^8D_{11/2}$	-3	3	-6	30
$4f^8 5d 6s^2\,{}^8G_{7/2}$	-2	-7	2	2
$4f^8 5d 6s^2\,{}^8D_{9/2}$	2	6	1	24
$4f^8 5d 6s^2\,{}^8G_{5/2}$	-1	1	2	8
$4f^8 5d 6s^2\,{}^8G_{3/2}$	0	0	3	-39
$4f^8 5d 6s^2\,{}^8F_{13/2}$	-1	0	-3	-23
$4f^8 5d 6s^2\,{}^8D_{7/2}$	0	-4	-2	-18
$4f^8 5d 6s^2\,{}^8G_{1/2}$	1	···	4	···
$4f^8 5d 6s^2\,{}^8H_{17/2}$	1	-3	3	8
$4f^8 5d 6s^2\,{}^8D_{5/2}$	1	18	-5	14

Table VI presents the results of the fits to the measured A and B values of 14 states in the $4f^8 5d 6s^2$ configuration. The 6-parameter fits are rather good; all A values are fitted to within 3%, and all B values but one to within 7%. The atom (in most states of this configuration) is so far removed from the LS limit[1,3] that no comparison with the limit is possible. The 2-parameter fit to the A values shows that all 14 A's are still fitted to within 6%. The corresponding fit to the B values, however, is apparently much less satisfactory; four B's differ by more than 20% from the calculated values. Comparison of Table VI with Table III shows, however, that the four states for which $B^{obs}-B^{calc}$ is relatively greatest are just those for which B is smallest; in fact, the absolute values of this difference for the four states are actually among the smaller ones. Table VII shows the contributions of the $4f$ and $5d$ shells to the B values separately, as calculated in the fit at the right in Table VI. It can be seen that the anomalously small B values found for the four states (${}^8D_{11/2},\,{}^8D_{9/2},\,{}^8G_{3/2}$, and ${}^8F_{13/2}$ in our designation) result from severe cancellation between the contributions of the two shells. The values found for the parameters in these fits will be discussed in Sec. IV J.

J. Quality of Fits and Parameter Values Obtained

Table VIII gives the parameter values obtained in making the 1- and 3-parameter fits to the A and

TABLE VII. Breakdown of B values for $4f^8 5d6s^2$ states into the portions arising from the $4f$ and $5d$ electron shells separately. Except for $^8G_{1/2}$, for which there can be no quadrupole hyperfine interaction, the four smallest B values (those for $^8D_{11/2}$, $^8D_{9/2}$, $^8G_{3/2}$, and $^8F_{13/2}$) result from severe cancellation between the two shells.

Configuration and state	B_f (MHz)	B_d (MHz)	$B^{calc} = B_f + B_d$ (MHz)
$4f^8 5d6s^2\ ^8G_{13/2}$	1224	-395	829
$4f^8 5d6s^2\ ^8G_{15/2}$	1076	-28	1048
$4f^8 5d6s^2\ ^8G_{11/2}$	1267	-414	853
$4f^8 5d6s^2\ ^8G_{9/2}$	1229	-34	1195
$4f^8 5d6s^2\ ^8D_{11/2}$	300	-365	-65
$4f^8 5d6s^2\ ^8G_{7/2}$	732	-13	719
$4f^8 5d6s^2\ ^8D_{9/2}$	278	-158	120
$4f^8 5d6s^2\ ^8G_{5/2}$	281	-36	245
$4f^8 5d6s^2\ ^8G_{3/2}$	14	-36	-22
$4f^8 5d6s^2\ ^8F_{13/2}$	128	-39	89
$4f^8 5d6s^2\ ^8D_{7/2}$	-128	-38	-166
$4f^8 5d6s^2\ ^8G_{1/2}$	0	0	0
$4f^8 5d6s^2\ ^8H_{17/2}$	1431	629	2060
$4f^8 5d6s^2\ ^8D_{5/2}$	-393	46	-347

B values of the $^6H_{15/2,\,13/2,\,11/2}$ states of $4f^9 6s^2$. The value found for a^{12} in the 3-parameter fit is unrealistically large. Although the ratio b_f^{13}/b_f^{11} has about the sign and magnitude expected from Eq. (12), the actual values found for b_f^{13} and b_f^{11} are much too large relative to b_f^{02}, and the discrepancy cannot be explained by invoking configuration interaction. The failure of the three measured B's to yield sensible values for the three parameters is accidental: The zero value of the reduced matrix element $\langle f^9\ ^6H \| V^{(13)} \| f^9\ ^6H \rangle$ leads to the result that in the LS limit no value of b_f^{13} is any better or worse than any other for fitting the observed B factors. Since the ^6H states are more than 94% pure, the value required for b_f^{13} is peculiarly sensitive to the exact nature of the admixture in the eigenvectors. The situation for determining the

TABLE VIII. Parameter values from the fits (Table V) to the hfs constants of ^6H states in the $4f^9 6s^2$ configuration. The values of a_{4f} and b_{4f} listed for the 3-parameter fits were obtained from a_f^{01} and b_f^{02}, respectively, by Eqs. (12).

Parameter	Parameter values (MHz)	
	3-parameter fits	1-parameter fits
a_f^{01}	1031	
a_f^{12}	1517	
a_f^{10}	-182	
a_{4f}	(1025)	959
b_f^{02}	2136	
b_f^{13}	3120	
b_f^{11}	-509	
b_{4f}	(2110)	2273

value of b_f^{11} is almost as unfavorable as a result of another accident: $B(^6H_{15/2})$ is exactly proportional to $B(^6H_{13/2})$, and almost exactly proportional to $B(^6H_{11/2})$ in the LS limit, regardless of b_f^{02}, b_f^{13}, or b_f^{11}.

It is believed that the values of the ratios a_f^{12}/a_f^{01}, b_f^{13}/b_f^{02}, and b_f^{11}/b_f^{02} estimated by use of Eq. (12), which follows from the Casimir factors, should be better than those found in the 3-parameter fits. The magnitude of a_f^{10}/a_f^{01} is more difficult to estimate because of the relatively large values sometimes caused by core-polarization effects. The values given for a_{4f} and b_{4f} in the 3-parameter fits are calculated from a_f^{01} and b_f^{02} by use of Eq. (12). The values found for a_{4f} and b_{4f} from the 1-parameter relativistic fits should be more realistic even though the fit itself, given in Table V, is not as good as might be expected for states that are 94% pure.

The failure of the 1-parameter theoretical expressions for A and B values of the $4f^9 6s^2\ ^6H$ states to fit the observed values better may most logically be attributed to imperfections in the intermediate-coupling eigenvectors[4] used. These eigenvectors were derived without experimental knowledge of the real energy spacings, and therefore must represent only a first approximation to the true eigenvectors. The eigenvectors of Conway and Wybourne[4] and of Judd and Lindgren[5] for the $^6H_{15/2,\,13/2}$ states both give calculated g_J values much closer to experiment than does the LS-coupling model, but neither set gives much improvement over the LS limit for $^6H_{11/2}$. It is curious that the 1-parameter relativistic fit to the A's is so much better than that for the B's. If one introduces a second parameter to allow for dipole core polarization of the $\vec{I} \cdot \vec{S}$ type, little improvement is found in the fit to the A's and the best value for the new parameter turns out to be very nearly zero.

The parameter values found for the 6- and 2-parameter fits to the A and B values of states in the $4f^8 5d6s^2$ configuration are summarized in Table IX. The value found for a_f^{12} is very slightly larger than that for a_f^{01}, as expected on the basis of relativity from Eq. (12), but configuration interaction can easily produce such small differences also. Similarly, a_f^{10} has the sign predicted by Eq. (12), but here again it is small and may well be due mostly to core polarization rather than relativity. However, the parameters associated with the $5d$ electron are much harder to understand. The values of a_d^{12}/a_d^{01} and a_d^{10}/a_d^{01} are both much larger than expected, and the sign of the latter disagrees with the prediction of Eq. (12). The value of a_d^{10} may well be due to configuration interaction (probably core polarization), but the size of a_d^{12} remains puzzling. The values obtained for a_{4f}

TABLE IX. Parameter values obtained in the fits (Table VI) to the A and B values of $4f^8 5d6s^2$ states in Tb^{159}. The values listed for a_{4f}, a_{5d}, b_{4f}, and b_{5d} in the 6-parameter fits were obtained from a_f^{01}, a_d^{01}, b_f^{02}, and b_d^{02}, respectively, by Eqs. (12).

Parameter	Parameter values (MHz)	
	6-parameter fits	2-parameter fits
a_f^{01}	1040	
a_f^{12}	1090	
a_f^{10}	− 38	
a_d^{01}	342	
a_d^{12}	139	
a_d^{10}	61	
a_{4f}	(1033)	1007
a_{5d}	(328)	340
b_f^{02}	2283	
b_f^{13}	1408	
b_f^{11}	− 806	
b_d^{02}	1272	
b_d^{13}	405	
b_d^{11}	− 278	
b_{4f}	(2255)	2117
b_{5d}	(1172)	1048

and a_{5d} from the 2-parameter fit (which is still) of high quality) should be realistic, and they are seen to be close to those obtained from a_f^{01} and a_d^{01} by application of Eq. (12).

The parameter values obtained in the fit to the quadrupole interaction constants are more difficult to understand. The expected signs are found for all six parameters, but b_f^{13} and b_f^{11} both appear unphysically large. The value found for b_d^{13}/b_d^{02} is almost exactly that predicted by Eq. (12), but b_d^{11} appears anomalously large. It is worth noting that the purely relativistic contribution $\vec{U}_d^{(13)2}$ to the quadrupole hyperfine constant B becomes very large (~ 30% of the nonrelativistic value) in an atom with such a large Z as Tb.

K. Interpretation of a_{nl} and b_{nl}, and the Electric-Quadrupole Moment of the Tb^{159} Nuclear Ground State

The electric-quadrupole moment Q of the nuclear ground state may be extracted from the measured value of b_{nl} by using the second of Eqs. (15) if the value of $\langle r^{-3} \rangle_{nl}$ is known. Since the value of a_{nl} is also measured, it is natural to use the first of Eqs. (15) to evaluate $\langle r^{-3} \rangle_{nl}$. Although the quantity $\langle r^{-3} \rangle_{nl}$ appears in both equations, care must be taken with regard to shielding effects. Dipole core-polarization effects are apparently very small in Tb, as shown by the excellent fits to the A values listed at the right in Tables V and VI, in which relativistic effects are explicitly included but core polarization is ignored. In addition, negligible improvement in these fits is obtained if an addition-

al parameter is introduced for each unfilled electron shell nl to take account of core polarization.

It has been shown by Sternheimer,[9] however, that shielding (or antishielding) effects in the quadrupole interaction can be large. In the equation $b_{nl} = e^2 Q \langle r^{-3} \rangle_{nl}$, in which b_{nl} has a measured value, the present interpretation is that $\langle r^{-3} \rangle_{nl}$ is the quantity that appears in expression (15) for a_{nl}, and that Q is an apparent quadrupole moment subject to correction by the Sternheimer correction factor. We may then more accurately rewrite the second of Eqs. (15) as

$$b_{nl} = e^2 Q'_{nl} \langle r^{-3} \rangle_{nl} \quad , \tag{16}$$

in which Q'_{nl} is the apparent nuclear-quadrupole moment, before correction for Sternheimer shielding, as determined from the electron shell nl. The correction factor may be expressed[9] in the form $1/(1 - R_{nl})$ so that we have

$$Q = [1/(1 - R_{nl})] Q'_{nl} \tag{17}$$

or, conversely,

$$Q'_{nl} = (1 - R_{nl}) Q \quad .$$

The quantity R_{nl} may be obtained theoretically.[9]
For the $4f^8 5d6s^2$ configuration, the ratio

$$a_{4f}/a_{5d} = \langle r^{-3} \rangle_{4f} / \langle r^{-3} \rangle_{5d} = \tfrac{1007}{340} = 2.96 \tag{18}$$

follows from the values of a_{4f} and a_{5d} found in the fits to the data. Similarly, using Eq. (16) instead of (15), we obtain

$$b_{4f}/b_{5d} = (\langle r^{-3} \rangle_{4f} / \langle r^{-3} \rangle_{5d}) \, Q'_{4f}/Q'_{5d} = \tfrac{2117}{1048} = 2.02 \quad . \tag{19}$$

Equations (18) and (19) can be consistent only if $Q'_{4f}/Q'_{5d} = 0.68$. Sternheimer[9,27] has estimated that $R_{4f} = +0.1 \pm 0.05$ and $R_{5d} = -0.3$, from which

$$Q'_{4f} = (1 - 0.1) Q = 0.90 Q \quad ,$$

$$Q'_{5d} = [1 - (-0.3)] Q = 1.30 Q \quad , \tag{20}$$

and consequently,

$$Q'_{4f}/Q'_{5d} = 0.69 \quad , \tag{21}$$

as required to satisfy Eqs. (18) and (19) simultaneously. Thus, the apparently small value found for b_{4f}/b_{5d} relative to a_{4f}/a_{5d} is just what is expected on the basis of the calculated values of the shielding factor R_{nl}.

If Eq. (16) is divided by the first of Eqs. (15), one obtains

$$\frac{b_{nl}}{a_{nl}} = \frac{e^2}{2\mu_B \mu_N} \frac{Q'_{nl}}{(\mu_I/I)} = \frac{e^2}{2\mu_B \mu_N} (1 - R_{nl}) \frac{Q}{(\mu_I/I)} \quad , \tag{22}$$

which shows that except for the Sternheimer correction factor $(1 - R_{nl})$, values of b_{nl}/a_{nl} should be independent of the electron shell nl. Table X compares the values obtained for this ratio under var-

TABLE X. Values of the ratio b_{nl}/a_{nl} as found from various fits to the A and B values of atomic levels in Tb[159]. In the upper half of the table, values of a_{nl} and b_{nl} resulting from fits to all observed states were used; in the bottom section, only those states believed most pure were considered. The values at the left are from fits allowing six free parameters per shell (three for the dipole fit, and three for the quadrupole), while those at the right result from fits allowing only two free parameters (one each for the dipole and quadrupole interactions). It is shown in the text that the value of b_{5d}/a_{5d} is expected to be about 45% larger than b_{4f}/a_{4f}, as is observed, because of the different Sternheimer shielding in the two shells.

Configuration	n and l of electron shell used	Value of b_{nl}/a_{nl} 6 parameters per shell	Value of b_{nl}/a_{nl} 2 parameters per shell
$4f^85d6s^2$	$4f$	2.18	2.10
$4f^85d6s^2$	$5d$	3.57	3.08
$4f^96s^2$	$4f$	2.06	2.37
$4f^85d6s^2$	$4f$	∘∘∘	2.34
$4f^85d6s^2$	$5d$	⋯∘	3.08
$4f^96s^2$	$4f$	⋯	2.46

ious conditions. In the top section of the table, the ratios given at the left (or right) follow from the fits at the left (or right) in Tables V, VI, VIII, and IX. Some of the parameters varied in making the fits at the left assumed unphysical values, as discussed in the text, and the resulting values of b_{nl} and a_{nl} may thereby have been affected. For this reason, it is felt that the results given for b_{nl}/a_{nl} at the right are probably more realistic physically. It is seen that the $4f$ electrons give nearly the same result whether in the $4f^85d6s^2$ or $4f^96s^2$ configuration, but the value obtained from the $5d$ shell in $4f^85d6s^2$ is considerably larger.

In an attempt to see if an appreciable part of the spread in the values in the upper half of Table X might be due primarily to imperfections in the eigenvectors, an effort was made to obtain the same information from those states for which the eigenvectors were believed best known, i.e., from states closest to the LS limit. For the $4f^96s^2$ configuration, the Conway-Wybourne[4] eigenvector for the lowest $^6H_{15/2}$ state was assumed perfect, and data on $^6H_{13/2}$ and $^6H_{11/2}$ was ignored. For $4f^85d6s^2$, the state of largest J ($^8H_{17/2}$) and of smallest J ($^8G_{1/2}$) – 97% and 94% pure, respectively, according to the Crosswhite eigenvectors[20] – were used alone to determine a_{4f} and a_{5d}. Since there is no quadrupole interaction for $^8G_{1/2}$, the state $^8G_{3/2}$ (nominally 89% pure) was used together with $^8H_{17/2}$ to determine b_{4f} and b_{5d}. The resulting ratios, presented in the bottom half of Table X, thus make use only of those states whose purity is high and

whose principal impurities are probably better known than for most of the states. The results are little changed from those in the top section of the table.

Equation (22) can be rearranged to yield the quadrupole moment Q as

$$Q = \frac{2\mu_B\mu_N}{e^2}\frac{\mu_I}{I}\frac{1}{1-R_{nl}}\left(\frac{b_{nl}}{a_{nl}}\right) = \frac{0.540}{1-R_{nl}}\left(\frac{b_{nl}}{a_{nl}}\right)b\ . \tag{23}$$

Or if the expressions are written separately for the two shells and Sternheimer's[27] estimates of R_{4f} and R_{5d} are used, the results are

$$Q = 0.599\left(\frac{b_{4f}}{a_{4f}}\right)b = 0.415\left(\frac{b_{5d}}{a_{5d}}\right)b\ . \tag{24}$$

When the results at the right of Table X are put into Eqs. (24), one finds from the $4f^96s^2$ configuration that

$$Q(\text{Tb}^{159};\ 4f^96s^2;4f) = +1.45(17)b\ , \tag{25}$$

where we have taken the mean of the values of b_{4f}/a_{4f} obtained from all three ^6H states (upper half of Table X) and that obtained from $^6H_{15/2}$ alone (bottom section). The uncertainty assigned to this value and to those that follow is a combination of the estimated uncertainty in b_{nl}/a_{nl} and that in the Sternheimer correction.

From the $4f^85d6s^2$ configuration, again taking the mean between the top and bottom parts of the table, we find from the $4f$ shell that

$$Q(\text{Tb}^{159};\ 4f^85d6s^2;4f) = +1.33(12)b\ , \tag{26}$$

and from the $5d$ shell that

$$Q(\text{Tb}^{159};4f^85d6s^2;5d) = +1.28(14)b\ . \tag{27}$$

These results are mutually consistent; the weighted average of the three separate determinations gives

$$Q(\text{Tb}^{159}) = +1.34(11)\ b\ , \tag{28}$$

where the uncertainty assigned has been increased over the statistical value to reflect the fact that the values of Q from Eqs. (26) and (27) are not completely independent. This value is in good agreement with most earlier measurements,[3,6,8] which range from 1.18 to 1.32 b.

Extraction of a value for Q depends on separating the roles played by the electrons and the nucleus in the measured quadrupole interaction energy. The accuracy of the value obtained for Q is directly tied to any error in understanding the electron part of the electron-nuclear quadrupole hyperfine-interaction energy. The present value of Q rests on a self-consistent understanding of the role played by two different electron shells in the quadrupole hfs of many different levels in two configurations.

It is felt that it should be more dependable than earlier results based on fitting fewer observations.

V. SUMMARY AND CONCLUSIONS

The present investigation was not able to determine whether the atomic ground state of Tb I is $4f^9 6s^2\, {}^6H_{15/2}$ or $4f^8 5d 6s^2\, {}^8G_{13/2}$ because of uncertainties in interpreting the observed relative intensities of rf transitions. Although detailed study of the hfs of the ${}^6H$ term of $4f^9 6s^2$ shows that the eigenvectors[4,5] need refinement, the high purity of the states nevertheless allows extraction of a dependable value for the electric-quadrupole moment Q of the Tb^{159} nuclear ground state. Eigenvectors computed for $4f^8 5d 6s^2$ with a severely truncated space are surprisingly good for the lower levels,[3,20] allow a detailed self-consistent interpretation of the observed hyperfine structure, and lead to a value of Q in good agreement with that obtained from $4f^9 6s^2$.

Although a great deal of quantitative information is obtained about the values of various atomic radial integrals (which are treated as free parameters in fitting routines), a number of problems remain unsolved. When allowed to vary freely, some of the parameter values (particularly a_l^{12}, b_l^{13}, and b_l^{11}) resulting from the fit are much larger than is physically reasonable.

It is hoped that the present results, both experimental and theoretical, will be of sufficient interest to theoretical atomic physicists to encourage them to make more comprehensive attempts to understand details of the observed hyperfine structure of Tb^{159}.

APPENDIX

The matrix element of the magnetic-dipole hyperfine-interaction operator $\mathcal{3C}_{hfs}\,(M1)$ of Eq. (6) is

$$\langle l^N \alpha_1 S_1 L_1, S_2 l'; SLJIFM | \mathcal{3C}_{hfs}(M1) | l^N \alpha_1' S_1' L_1', S_2 l'; S'L'J'IFM \rangle$$

$$= \Gamma_1(JJ'IF)\Bigg[\delta(\alpha_1 S_1 L_1, \alpha_1' S_1' L_1')\, \delta(S,S')\,(-1)^{S+L'+J+L_1+l'}$$

$$\times [(2L+1)(2L'+1)]^{1/2} \begin{Bmatrix} J & J' & 1 \\ L' & L & S \end{Bmatrix} \left(a_l^{01} \begin{Bmatrix} L & L' & 1 \\ L_1' & L_1 & l' \end{Bmatrix} (-1)^{L'}[L_1(L_1+1)(2L_1+1)]^{1/2} + a_{l'}^{01} \begin{Bmatrix} L & L' & 1 \\ l' & l' & L_1 \end{Bmatrix} \right.$$

$$\left. \times (-1)^L [l'(l'+1)(2l'+1)]^{1/2} \right) + [30(2L+1)(2L'+1)(2S+1)(2S'+1)]^{1/2} \begin{Bmatrix} S & S' & 1 \\ L & L' & 2 \\ J & J' & 1 \end{Bmatrix}$$

$$\times (-1)^{S_1+L_1+l'+S_2+1} \left(a_l^{12}(-1)^{S'+L'} \begin{Bmatrix} S & S' & 1 \\ S_1' & S_1 & S_2 \end{Bmatrix} \begin{Bmatrix} L & L' & 2 \\ L_1' & L_1 & l' \end{Bmatrix} \frac{[l(l+1)(2l+1)]^{1/2}}{[(2l-1)(2l+3)]^{1/2}} \right.$$

$$\times \langle l^N \alpha_1 S_1 L_1 \| V^{(12)} \| l^N \alpha_1' S_1' L_1' \rangle + a_{l'}^{12}\, \delta(\alpha_1 S_1 L_1, \alpha_1' S_1' L_1')(-1)^{S+L} \begin{Bmatrix} S & S' & 1 \\ S_2 & S_2 & S_1 \end{Bmatrix} \begin{Bmatrix} L & L' & 2 \\ l' & l' & L_1 \end{Bmatrix}$$

$$\left. \times \frac{[3l'(l'+1)(2l'+1)]^{1/2}}{[2(2l'-1)(2l'+3)]^{1/2}} \right) + \delta(\alpha_1 S_1 L_1, \alpha_1' S_1' L_1')\, \delta(L, L')(-1)^{S+J'+L+S_1+S_2}[(2S+1)(2S'+1)]^{1/2}$$

$$\times \begin{Bmatrix} J & J' & 1 \\ S' & S & L \end{Bmatrix} \left(a_{l}^{10}(-1)^{S'} \begin{Bmatrix} S & S' & 1 \\ S_1 & S_1 & S_2 \end{Bmatrix} [S_1(S_1+1)(2S_1+1)]^{1/2} + a_{l'}^{10}(-1)^{S} \begin{Bmatrix} S & S' & 1 \\ S_2 & S_2 & S_1 \end{Bmatrix} (\tfrac{3}{2})^{1/2} \right) \Big] \tag{A1}$$

for configurations either of the type $l^N l'$ or l^N. When Eq. (A1) is used for evaluation of matrix elements within configurations of the type $l^N l'$ (such as $4f^8 5d 6s^2$, for example), one sets $S_2 = \tfrac{1}{2}$. When dealing with l^N (such as $4f^9 6s^2$), one sets $S_2 = l' = 0$; $S_1, L_1 = S, L$; $S_1', L_1' = S', L'$; and $a_{l'}^{ks,kl} = 0$. In Eq. (A1), we have

$$\Gamma_1(JJ'IF) = (-1)^{J' + I + F} \begin{Bmatrix} J & J' & 1 \\ I & I & F \end{Bmatrix} [I(I+1)(2I+1)(2J+1)(2J'+1)]^{1/2} . \tag{A2}$$

Comparison of Eq. (A1) with the first term of Eq. (2) is greatly facilitated by noting that

$$\Gamma_1(JJIF) = \langle FM | \mathbf{I} \cdot \mathbf{J} | FM \rangle \{(2J+1)/[J(J+1)]\}^{1/2} . \tag{A3}$$

By combining Eqs. (A1) and (A3), the proper expression for the generalized A factor between any two LS basis states can be read off in terms of the parameters $a_l^{ks,kl}$ and $a_{l'}^{ks,kl}$.

In analogy to Eq. (A1), the matrix element of the electric-quadrupole hyperfine operator $\mathcal{K}_{hfs}$ (E2) of Eq. (7) is

$$\langle l^N \alpha_1 S_1 L_1, S_2 l'; SLJIFM | \mathcal{K}_{hfs} (E2) | l^N \alpha_1' S_1' L_1', S_2 l'; S'L'J'IFM \rangle$$

$$= \Gamma_2(JJ'IF) \Bigg\{ \begin{Bmatrix} J & J' & 2 \\ L' & L & S \end{Bmatrix} \delta(S, S') \frac{(-1)^{S + L' + J + S' + 2S_2 + S_1 + l'}}{(10)^{1/2}(2S+1)} \left(\frac{[2l(l+1)(2l+1)]^{1/2}}{[(2l-1)(2l+3)]^{1/2}} \right.$$

$$\times b_l^{02} (-1)^{L' + S'} \begin{Bmatrix} L & L' & 2 \\ L_1' & L_1 & l' \end{Bmatrix} \delta(S_1, S_1') \langle l^N \alpha_1 S_1 L_1 \| U^{(2)} \| l^N \alpha_1' S_1' L_1' \rangle + b_{l'}^{02}$$

$$\times \frac{[2l'(l'+1)(2l'+1)]^{1/2}}{[(2l'-1)(2l'+3)]^{1/2}} \delta(\alpha_1' S_1 L_1, \alpha_1' S_1' L_1')(-1)^{L+S} \begin{Bmatrix} L & L' & 2 \\ l' & l' & L_1 \end{Bmatrix} \Bigg) + (5)^{-1/2} \begin{Bmatrix} S & S' & 1 \\ L & L' & 3 \\ J & J' & 2 \end{Bmatrix}$$

$$\times \left[b_l^{13} (-1)^{S_2 + l' + S' + L'} \begin{Bmatrix} S & S' & 1 \\ S_1' & S_1 & S_2 \end{Bmatrix} \begin{Bmatrix} L & L' & 3 \\ L_1' & L_1 & l' \end{Bmatrix} \langle l^N \alpha_1 S_1 L_1 \| V^{(13)} \| l^N \alpha_1' S_1' L_1' \rangle + b_{l'}^{13} \delta(\alpha_1 S_1 L_1, \alpha_1' S_1' L_1') \right.$$

$$\times (-1)^{S_2 + l' + S + L} \left(\frac{3}{2} \right)^{1/2} \begin{Bmatrix} S & S' & 1 \\ S_2 & S_2 & S_1 \end{Bmatrix} \begin{Bmatrix} L & L' & 3 \\ l' & l' & L_1 \end{Bmatrix} \Bigg] + (5)^{-1/2} \begin{Bmatrix} S & S' & 1 \\ L & L' & 1 \\ J & J' & 2 \end{Bmatrix}$$

$$\times \left[b_l^{11} \begin{Bmatrix} S & S' & 1 \\ S_1' & S_1 & S_2 \end{Bmatrix} \begin{Bmatrix} L & L' & 1 \\ L_1' & L_1 & l' \end{Bmatrix} (-1)^{S_2 + l' + S' + L'} \langle l^N \alpha_1 S_1 L_1 \| V^{(11)} \| l^N \alpha_1' S_1' L_1' \rangle + b_{l'}^{11} \delta(\alpha_1 S_1 L_1, \alpha_1', S_1', L_1') \right.$$

$$\times (-1)^{S_2 + l' + S + L} \begin{Bmatrix} S & S' & 1 \\ S_2 & S_2 & S_1 \end{Bmatrix} \begin{Bmatrix} L & L' & 1 \\ l' & l' & L_1 \end{Bmatrix} \left(\frac{3}{2} \right)^{1/2} \Bigg] \Bigg\} , \tag{A4}$$

where the $b_{l'}^{ks,kl}$ are zero for matrix elements within configurations of the type l^N. In Eq. (A4),

$$\Gamma_2(JJ'IF) = (-1)^{J' + I + F + S_1 + L_1} \begin{Bmatrix} J & J' & 2 \\ I & I & F \end{Bmatrix} \frac{1}{2} \left(\frac{(2I+3)(I+1)(2I+1)}{I(2I-1)} \right)^{1/2}$$

$$\times [5(2J+1)(2J'+1)(2S+1)(2S'+1)(2L+1)(2L'+1)]^{1/2} . \tag{A5}$$

The expression analogous to Eq. (A3) may be written

$$\Gamma_2(JJIF) = \langle FM | Q_{op} | FM \rangle (-1)^{S_1 + L_1} 2[5(2S+1)(2S'+1)(2L+1)(2L'+1)]^{1/2} \left(\frac{J(2J-1)(2J+1)}{(J+1)(2J+3)} \right)^{1/2} , \tag{A6}$$

in which[13]

$$\langle FM | Q_{op} | FM \rangle = [\tfrac{3}{4}K(K+1) - I(I+1)J(J+1)]/2 I(2I-1)J(2J-1) \tag{A7}$$

and[13] $K \equiv 2\langle FM| \vec{I} \cdot \vec{J} |FM\rangle = F(F+1) - I(I+1) - J(J+1)$.   (A8)

The generalization of the electronic part of the Zeeman interaction, Eq. (3), may be written for calculations in the LS scheme as

$$\mathcal{3C}_z^{el} = \mu_0 \vec{H} \cdot (\vec{L} + g_s \vec{S}) ,$$ (A9)

where $g_s = 2.00232$.   (A10)

Its matrix element, which is diagonal in S and L but not necessarily in J or F, is

$$\langle l^N \alpha_1 \; S_1 L_1, S_2 l'; SLJIFM | \mathcal{3C}_z^{el} | l^N \alpha_1' S_1' L_1', S_2 l'; S'L'J'IF'M\rangle$$

$$= \delta(\alpha_1 S_1 L_1, \alpha_1' S_1' L_1') \; \delta(S,S') \delta(L,L') \mu_0 H \begin{pmatrix} F' & F & 1 \\ M & -M & 0 \end{pmatrix} \begin{Bmatrix} F'F & 1 \\ J & J' & I \end{Bmatrix}$$

$$\times [(2J+1)(2J'+1)(2F+1)(2F'+1)]^{1/2} (-1)^{J+I+F'-M+S+L+F}$$

$$\times \left(g_s(-1)^{J'} \begin{Bmatrix} J & J' & 1 \\ S & S & L \end{Bmatrix} [S(S+1)(2S+1)]^{1/2} + (-1)^J \begin{Bmatrix} J & J' & 1 \\ L & L & S \end{Bmatrix} [L(L+1)(2L+1)]^{1/2} \right) .$$ (A11)

The relativistic correction factors whose numerical values were given for Tb in Eq. (12) may be easily calculated from the Casimir factors. Expressions relating the quantities $b_l^{ks, kl}$ to b_{nl} have been published.[23] The corresponding expressions for the $a_l^{ks, kl}$ are

$$a_l^{01} = a_{nl}(2l+1)^{-2}[2l(l+1)F_r(l+\tfrac{1}{2}, Z_{eff}) + 2l(l+1)F_r(l-\tfrac{1}{2}, Z_{eff}) + G_r(l, Z_{eff})] ,$$

$$a_l^{12} = (\tfrac{1}{3}a_{nl})(2l+1)^{-2}[-4l(l+1)(2l-1)F_r(l+\tfrac{1}{2}, Z_{eff}) + 4l(l+1)(2l+3)F_r(l-\tfrac{1}{2}, Z_{eff}) - (2l+3)(2l-1)G_r(l, Z_{eff})] ,$$ (A12)

$$a_l^{10} = (\tfrac{1}{3}4a_{nl})l(l+1)(2l+1)^{-2}[(l+1)F_r(l+\tfrac{1}{2}, Z_{eff}) - l F_r(l-\tfrac{1}{2}, Z_{eff}) - G_r(l, Z_{eff})] ,$$

in which the quantities $F_r(l \pm \tfrac{1}{2}, Z_{eff})$ and $G_r(l, Z_{eff})$ are the Casimir[24] factors. The quantities a_l^{01} and a_l^{12} approach a_{nl} and a_l^{10} approaches zero in the nonrelativistic limit if configuration-interaction effects are ignored. In the quadrupole interaction, b_l^{02} approaches b_{nl}, but b_l^{13} and b_l^{11} both approach zero in the nonrelativistic limit, regardless of configuration-interaction effects.

---

*Work performed under the auspices of the U.S. Atomic Energy Commission.

[1]E. Meinders and P. F. A. Klinkenberg, Physica 32, 1113 (1966); 32, 1617 (1966); 37, 197 (1967); 38, 253 (1968).

[2]I. Bender, S. Penselin, and K. Schlupmann, Z. Physik 179, 4 (1964).

[3]C. Arnoult and S. Gerstenkorn, J. Opt. Soc. Am. 56, 177 (1966); Compt. Rend. 261, 1488 (1965).

[4]J. G. Conway and B. G. Wybourne, Phys. Rev. 130, 2325 (1963). Several errors in the eigenvectors were corrected by Conway (private communication).

[5]B. R. Judd and I. Lindgren, Phys. Rev. 122, 1802 (1961).

[6]K. H. Chan and P. J. Unsworth (private communication).

[7]J. M. Baker, J. R. Chadwick, G. Garton, and J. P. Hurrell, Proc. Roy. Soc. (London) 286, 352 (1965).

[8]G. H. Fuller and V. W. Cohen, in Nuclear Data Tables,

edited by K. Way (Academic, New York, 1969), p. 433. A new measurement of Q is reported by P. F. A. Klinkenberg and J. W. M. Dekker, Physica 43, 92 (1969).

[9]R. M. Sternheimer, Phys. Rev. 146, 140 (1966); 164, 10 (1967).

[10]W. J. Childs and L. S. Goodman, Bull. Am. Phys. Soc. 14, 84 (1969); J. Opt. Soc. Am. 59, 875 (1969).

[11]I. I. Rabi, J. R. Zacharias, S. Millman, and P. Kusch, Phys. Rev. 53, 318 (1938); J. R. Zacharias, ibid. 61, 270 (1942).

[12]See, for example, W. J. Childs, L. S. Goodman, and D. von Ehrenstein, Phys. Rev. 132, 2128 (1963).

[13]N. F. Ramsey, Molecular Beams (Oxford U.P., New York, 1956), pp. 272, 277.

[14]These programs are adaptations of routines kindly supplied by H. Shugart of the University of Calif., Berkeley.

[15]The data-handling system has been described in more detail by W. J. Childs and L. S. Goodman, Phys. Rev.

<u>148</u>, 74 (1966).

[16]L. S. Goodman and F. O. Salter, Rev. Sci. Instr. <u>37</u>, 769 (1966).

[17]N. F. Ramsey, Ref. 13, Chap. V; W. J. Childs, L. S. Goodman, and L. J. Kieffer, Phys. Rev. <u>122</u>, 891 (1961).

[18]B. G. Wybourne, *Spectroscopic Properties of Rare Earths* (Interscience, New York, 1965), p. 3.

[19]C. W. Nielson and G. F. Koster, *Spectroscopic Coefficients for the p^n, d^n, and f^n Configurations* (MIT U. P., Cambridge, Mass., 1963).

[20]H. Crosswhite (private communication).

[21]P. G. H. Sandars and J. Beck, Proc. Roy. Soc. (London) <u>A289</u>, 97 (1965).

[22]B. R. Judd, J. Math. Phys. <u>3</u>, 557 (1962).

[23]W. J. Childs and L. S. Goodman, Phys. Rev. <u>170</u>, 50

(1968).

[24]Tables of the Casimir factors for p and d electrons, and formulas for extending the calculations to f electrons, are given by H. Kopfermann, *Nuclear Moments*, translated by E. E. Schneider (Academic, New York, 1958), pp. 445–449.

[25]See, for example, G. K. Woodgate, Proc. Roy. Soc. (London) <u>A293</u>, 117 (1966); W. J. Childs, Phys. Rev. <u>156</u>, 71 (1967).

[26]This is a generalization of a result given by W. J. Childs, Phys. Rev. <u>156</u>, 71 (1967).

[27]R. M. Sternheimer (private communication). Both of these values are slightly smaller in magnitude than those of Ref. 9 because the latter calculations did not take account of exchange effects.

Coherent Spontaneous Emission*

Rodolfo Bonifacio†

and

Giuliano Preparata‡

Lyman Laboratory of Physics, Harvard University, Cambridge, Massachusetts 02139

(Received 16 June 1969)

Coherent spontaneous emission from a system of N two-level atoms interacting with a quantized radiation field is treated for the case in which Dicke's "cooperation number" r is macroscopically large. It is shown how to modify the quasiclassical approach to this problem to incorporate quantum effects that are lost in the self-consistent-field approximation. The statistics of the emitted radiation are found to vary markedly with the initial state of the system of atoms. The photon statistics tend to that typical of blackbody radiation when the initial state of the atomic system is that which would result from incoherent pumping $(m \sim r)$. When, on the other hand, the atoms are initially in a superradiant state $(m \ll r)$, the emitted radiation may be represented approximately by a coherent state.

I. INTRODUCTION

Several years ago Dicke[1] introduced the concept of coherence in spontaneous radiative emission from a system of N "molecules" which undergo transitions between two energy levels. In this paper we present a detailed discussion of a recent paper of ours,[2] in which a nonperturbative solution of the problem has been given.

The main feature of coherent spontaneous radiation processes is the possibility, in certain configurations, of having the radiation rate proportional to N^2 rather than to N, as one would expect when the molecules radiate "incoherently," i.e., independently of each other. Such an anomalously large radiation rate occurs as a consequence of a highly correlated motion of the N-molecules system, which, as a consequence, radiates as a single quantum-mechanical system. These exception-

al states were called superradiant states by Dicke. They belong to a class of correlated states of the N-molecules system which are best defined in the framework of angular momentum theory.[3]

By representing the single two-energy-level molecule as a spin-$\frac{1}{2}$ particle, one can define a "superradiant" state as a particular eigenstate of the *total* angular momentum $|r, m\rangle$. The total angular momentum quantum number r was called the "cooperation" number by Dicke, and is obviously related to the degree of correlation among the spins.

On the other hand, $m = \frac{1}{2}(n_+ - n_-)$ $(n_+, n_-$ give the number of excited and nonexcited molecules, respectively) is proportional to the energy stored in the system, and is such that $|m| \le r \le \frac{1}{2}N$.

Obviously the $|r, m\rangle$ states are not a complete basis for the N-spin system. However, from degeneracy considerations, Dicke[1] has shown that, if